ENVIRONMENTALLY-ASSISTED DEGRADATION OF STAINLESS STEELS IN LWRs

Environmentally-Assisted Degradation of Stainless Steels in LWRs

Authors

F. Peter Ford
Rexford, NY, USA

Peter M. Scott
Noisy Le Roi, France

Pierre Combrade
Le Bessat, France

A.N.T. INTERNATIONAL®

Advanced Nuclear Technology International
Krongjutarvägen 2C, SE-730 50 Skultuna
Sweden

info@antinternational.com
www.antinternational.com

green print

Disclaimer

The information presented in this report has been compiled and analysed by Advanced Nuclear Technology International Europe AB (ANT International®) and its subcontractors. ANT International has exercised due diligence in this work, but does not warrant the accuracy or completeness of the information. ANT International does not assume any responsibility for any consequences as a result of the use of the information for any party, except a warranty for reasonable technical skill, which is limited to the amount paid for this Report.

Contents

Executive summary

This report is the third in a series of Special Topical Reports (STR) covering environmentally-assisted degradation of structural materials in water cooled reactors.

The first, issued in 2006, was an introduction to the topic and was intended for readers who were new to the subject, or needed updates on topics such as the basics of corrosion, the reasons for the choice of various alloys commonly used in construction, the mechanisms of various degradation modes, and the various mitigation actions that have been applied in Boiling and Pressurized Water Reactors (PWRs). The second STR, issued in 2008, concentrated on degradation modes that were specific to carbon and low alloy steel. This third report focuses on various degradation modes for stainless steels such as pitting, crevice corrosion and Stress Corrosion Cracking (SCC).

The overall objective of this report is to describe the numerous occurrences of environmentally-assisted degradation that have occurred in stainless steels since the late 1950s in water-cooled reactors. Emphasis is placed on an understanding of the reactor operating conditions that promote such degradation. This, combined with an adequate understanding of the mechanisms of these degradation phenomena, leads to the definition of operating conditions that ensure minimal frequency of occurrence in the future.

In order to meet this overall objective, this report have been organized in the following subject areas:

- **The physical metallurgy of stainless steels**, since this knowledge is necessary when discussing the various embrittlement and degradation modes.

- **The corrosion basics of stainless steels,** since general corrosion resistance was a prime reason for their choice as a structural material. Moreover, the water chemistry specifications required for this resistance in Light Water Reactors (LWRs) have a bearing on susceptibility to various localized degradation modes.

- **SCC of stainless steels in BWRs**, since such cracking in the primary coolant system was, historically, the initial major concern related to environmental degradation effects on the structural integrity of stainless steel piping. Note that, subsequently, this initial concern was expanded to cover cracking of stainless steels in reactor internals exposed to high irradiation fluxes and those in cold worked conditions.

- **SCC of stainless steels in PWR-type coolants** since this is a more recent phenomena that highlights the fact that "cracking resistance" is determined by the conjunction of many different system parameters, and the "unexpected" imposition of other parameters (e.g. excessive cold work and substantial irradiation damage) may jeopardize that resistance.

- **Corrosion of stainless steels in contaminated environments** usually associated with secondary and tertiary systems or in dead legs with non-optimum water chemistry in primary coolant systems. External surface corrosion due mainly to chloride contamination, often from thermal insulation materials, is another common cause of environmentally assisted degradation.

- **Corrosion fatigue** since, although fatigue is part of the original design criteria, the effect of the environment on crack initiation and propagation is not explicitly taken into account in the design process.

1 Introduction and background (Peter Ford)

1.1 Objective and Scope of Report

This report is the third in a series of topical reports covering environmentally-assisted degradation of structural materials in water-cooled nuclear reactors. The first in the series [Ford, 2006] served as an introduction to the subject and was aimed at personnel who either were new to the topic or needed a "refresher-course" on the underlying principles of uniform and localized corrosion phenomena relevant to water-cooled nuclear reactors. The second report [Ford & Scott, 2008] in the series used the 2006 report as a base and focused in more detail on the environmentally-assisted degradation of carbon and low–alloy steels. This third report focuses on various degradation modes for stainless steels such as pitting, crevice corrosion and SCC. A significant amount of attention is given to Environmentally-Assisted Cracking (EAC) in both Boiling Water (BWR) and PWRs, since EAC has posed significant economic and potential safety issues over the years.

The nuclear industry has developed mitigation actions and aging management programmes to deal with materials degradation problems. However, these activities, and the associated actions by the regulators, have usually been conducted *after* the incidents have occurred. This reactive nature of the response has had two major consequences. First, if the integrity of the plant and its safety barriers cannot be demonstrated to an acceptable level, then the plant is shut down or proceeds at reduced power until repairs can be effected and/or mitigation actions developed and justified. This development can take a considerable time with accompanying high cost of lost production, especially since it also involves arriving at agreement with the regulator on the appropriate quantitative control criteria. Second, there are unplanned monetary and time commitments due to the unpredicted nature of the incidents.

Consequently, there has been a drive internationally to develop the capability to manage these materials degradation problems proactively and to move towards a mindset that not only *prevents* the degradation, but also *predicts* future degradation. That is, to identify a problem well before costly and potentially safety-significant incidents occur and, thereby, give a more extended time to develop mitigation and inspection strategies. A comparison between the reactive and proactive management strategies for dealing with materials degradation issues is illustrated schematically in Figure 1-1 in which two examples of the development of damage are shown. In one case (shown by the left hand curve in Figure 1-1) the damage has developed to a point where it is detectable "now". That is, the extent of damage is greater than the resolution limit of the Non-Destructive Examination (NDE) procedure. In the absence of a mitigation action that can be immediately applied, it is expected that the damage will continue to develop and will eventually reach an unacceptable level, depending on some structural integrity criterion. It follows, therefore, that under such a reactive management mode there is a limited time for the development, qualification and approval of a sound mitigation plan. On the other hand it may well be that damage has not been detected "now" (i.e. the second example shown in Figure 1-1), but there is enough knowledge of the mechanism of degradation to predict that damage will be detected at a defined time in the future. If such a prediction capability existed then there would be two major advantages. First, there would be a considerably longer time for the development of mitigation actions and/or repair procedures, and second, there would be a logical format to prioritize the use of development funds to the problems that present the greatest risk.

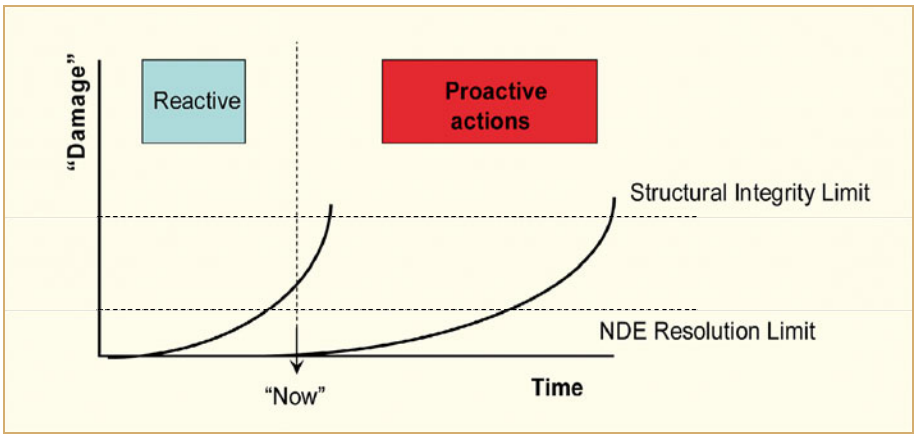

Figure 1-1: Schematic diagram illustrating degradation "damage" with time, and the differentiation between reactive and proactive actions. Note that the degradation process vs. time is rarely linear, as is often assumed. Note also that in the reactive mode, damage has been detected "now" and there is limited time for mitigation development before the structural integrity limit is reached. This development time is considerably increased in the proactive mode. (NDE=Non Destructive Examination) [Muscara, 2007].

The overall objective of this report is to describe the numerous occurrences of environmentally-assisted degradation that have occurred in stainless steels since the late 1950s in Water-Cooled Reactors. The near term objective is to assess the current knowledge that is sufficient to adequately predict, manage and regulate such phenomena. A longer-term objective is to develop a life prediction algorithm that is the central tool in a "monitoring and diagnostics" capability (Figure 1-2). Such a capability would give (a) a continuous, quantitative evaluation of the risk of degradation, together with the approaches that could be taken to minimize that risk and, (b) supplement the current approach of making decisions based solely on intermittent inspections during refuelling, or forced, outages. This broader, longer-range objective is addressed in a combined United States Nuclear Regulatory Commission (USNRC)/DOE programme (http://pmmd.pnl.gov/).

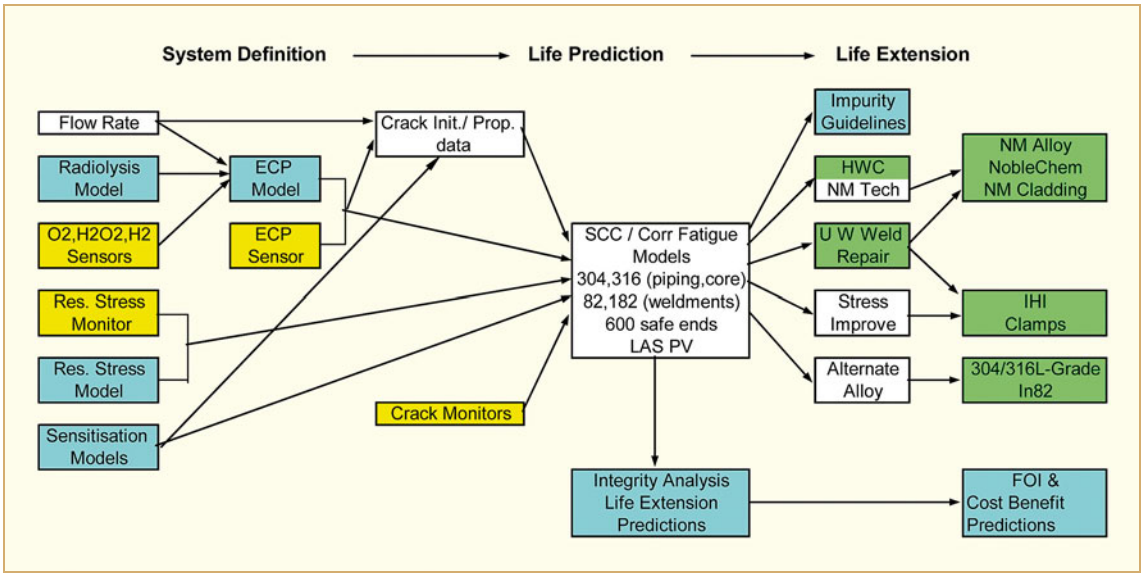

Figure 1-2: A monitoring and diagnostics scheme for managing SCC of stainless steels in BWRs [Ford et al, 1988] and [Ford et al, 1989].

The relevant inputs to such a monitoring and diagnostics scheme would include, for example, residual stress, materials sensitization and corrosion potential models and measurements, plus the associated "local to global" algorithms that expand the input information to unmonitored regions in the plant. The life prediction model for the specific degradation mode and material of construction should be based on sound laboratory and past plant experience, backed up by a quantitative understanding of the mechanism of cracking that is sufficient to explain the sensitivities of the relevant system parameters and their interactions. The outputs from the prediction model include the current and projected extents of damage, together with quantitative guidance on the timely and economic use of various mitigation actions.

In order to meet these objectives this report has been organized in the following logical order:

- The physical metallurgy of stainless steels, since this knowledge is necessary when discussing the various embrittlement and degradation modes.
- The corrosion basics of stainless steels, since general corrosion resistance was a prime reason for their choice as a structural material; note that the chemistry specifications required for this resistance have a bearing on the susceptibility to various localized degradation modes.
- SCC of stainless steels in BWRs, since such cracking in the primary system was, historically, the initial major concern related to environmental effects on structural integrity.
- SCC of stainless steels in PWR-type coolants since this is a more recent phenomena that highlights the fact that "cracking resistance" is determined by the conjunction of many different system parameters, and the "unexpected" imposition of one of these parameters (e.g. excessive cold work) may jeopardize that resistance.
- Corrosion of stainless steels in contaminated environments usually associated with secondary and tertiary systems or in "occluded conditions" with non-optimum water chemistry in primary coolant systems or on external surfaces due to contamination by pollutants.
- Corrosion fatigue since, although fatigue is part of the original design criteria, the effect of the environment on crack initiation and propagation is not explicitly taken into account in the design process.

1.2 Overview of environmentally-assisted degradation of stainless steels

Stainless steels are widely used in the primary circuits because of their mechanical and general corrosion resistance properties, as will be discussed in Chapters 1 and 3. For example, these steels are used as a cladding for the less corrosion resistant low alloy steel pressure vessel and, because of their tensile and fracture resistance properties, as pressure retaining boundary components, such as piping, and for core internal support structures. They can also serve as cladding of absorber rods and structural parts of control elements in the highest flux regions of the core.

Although these alloys have good general corrosion resistance they can be susceptible to localized corrosion degradation modes, as will be discussed in detail later in this report. For example, environmentally-assisted degradation problems with wrought austenitic stainless steels and their weldments have been experienced in water-cooled reactor service and include the following:

- Intergranular stress corrosion of sensitized piping exposed to oxygenated reactor coolant water in direct cycle BWRs where oxygen (plus hydrogen peroxide and oxidizing radicals) is generated by radiolysis. The cracking is associated with thermally activated grain boundary sensitization during furnace heat treatment or during welding. The tensile stress for the cracking originates from fit-up operations, pressurization stresses and weld residual stresses. The cracking of the sensitized structure is accelerated by a variety of system variables including surface cold work, anionic impurities, temperature, dynamic loading and the presence of oxidizing agents that raise the corrosion potential. This particular form of cracking has now been mitigated by a variety of actions discussed in detail in Chapter 4.

- Intergranular Stress Corrosion Cracking (IGSCC) of austenitic steels in irradiated BWR core environments where the affected core internals include the core shroud, its support structure and control rod assemblies. This phenomenon is an extension of the cracking observed in unirradiated piping. However, Irradiation Assisted Stress Corrosion Cracking (IASCC) is usually addressed as a separate topic from these earlier experiences since it introduces complicating factors associated with fast neutron flux and fluence, which can simultaneously change several variables in the cracking process. This broadens the system conditions under which the degradation is noted in service, and complicates the mitigation action options. These issues will be discussed in detail in Chapter 5.

- Both transgranular and IGSCC of irradiated and unirradiated stainless steels in PWRs in, for example, the deadlegs of primary circuits. These are unusual since the less oxidizing PWR primary environment would normally preclude such cracking. These incidents are discussed in Chapter 6.

- Pitting and transgranular SCC of stainless steel piping in both BWRs and PWRs at relatively low temperatures (i.e. < 100 °C). Such cracking may initiate on the *outside* of the pipe when exposed to a chloride contaminated environment (from, for example, airborne aerosols at marine sites, or contaminants in the thermal insulation). Similar occurrences have been noted on the inside of piping under dry lay-up conditions when the residual water in the system has been contaminated with chlorides. Another degradation mode in this category of failure in contaminated environments is microbiologically influenced corrosion (MIC) of austenitic steels that occurs especially in the weld regions in service and raw water and on external surfaces of buried piping. This may lead to localized corrosion and penetration of safety-significant components due mainly to pitting. Such incidents are discussed in Chapter 6.

- Fatigue failures of small diameter piping in both PWRs and BWRs, with uncertain contributions of the environment. As with the carbon and low alloy steels discussed in the LCC4 STR, these failures are associated with vibratory stresses and with thermal stresses due to flow eddies in deadlegs. Higher frequency (acoustic) vibrational loads, such as those experienced in some designs of BWR steam driers operating under power uprate conditions have led to premature failures; however it is unlikely in these high frequency conditions that there is a significant environmental component. These aspects are discussed in Chapter 7.

- Cracking of the stainless steel weld materials and cladding in BWRs is relatively rare because the ferrite in the duplex stainless steel microstructures tends to arrest crack propagation. However, there have been isolated occurrences normally associated with low ferrite contents in combination with the application of post weld heat treatments that sensitized the microstructure and oxidizing environmental conditions at the outlet of the reactor core. In some of these cases there has also been the possibility that these cracks in the cladding penetrated into the underlying low alloy steel, but in light of the marked resistance of the low alloy steel to SCC, such penetrations into the underlying materials have usually been attributed to "underclad cracking"[1].

[1] "Underclad cracking" is a degradation mode that is outside the scope of this report since its root cause is not specifically associated with the operating environment. The driving forces are related to the fabrication conditions that give rise to hot cracking (sometimes called liquation cracking), reheat cracking or cold cracking. The mechanisms of these three forms of cracking are different, and the rate controlling parameters are known. Consequently, mitigation actions have been implemented, and future environmental effects are unlikely to reintroduce these problems in the future.

2 Physical metallurgy of stainless steels (Peter Ford)

The compositions of the stainless steels reside primarily in the iron corner of the Fe-Cr-Ni ternary equilibrium diagram (Figure 2-1) and form an intermediate class of materials between the ferritic carbon and low alloy steels used for the pressure vessel and secondary piping systems, and the fully austenitic nickel-base alloys such as X718, X750, 600, 690, 182, 82, etc.[2]

Stainless steels are widely used in primary circuits of LWRs (as piping, pump casings, core internals, etc.) primarily because of their good general corrosion resistance due to the > 11% chromium content, and the wide variety of mechanical properties that can be achieved by compositional control and heat treatment. Moreover, these steels may be fabricated in a variety of wrought products such as plate and piping, as well as castings, cladding and weldments. The most commonly used stainless steel "family" is based on the Fe-18%Cr-10% nickel composition (Type 304 stainless steel) with further alloying elements being made (Figure 2-2) for specific property changes associated with control of grain boundary sensitization, precipitation hardening, ease of machining, pitting resistance, etc.

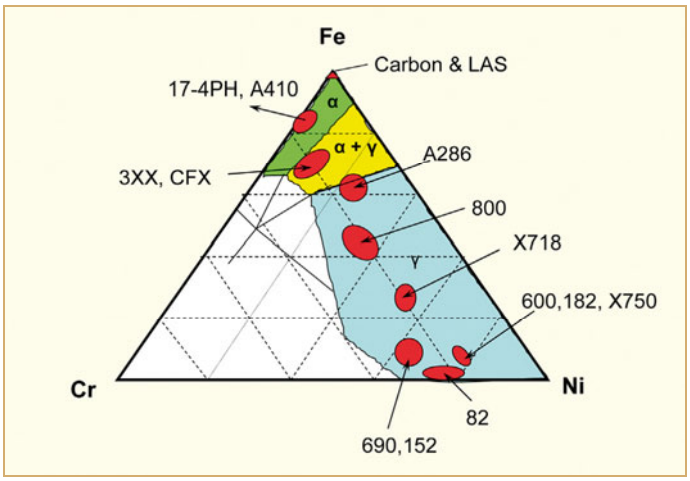

Figure 2-1: Simplified Ternary Equilibrium Diagram for Iron, Chromium and Nickel at 400 °C.

The wrought stainless steels may be classified in terms of their crystal structure, (austenitic, ferritic, martensitic and duplex), as well as their ability to achieve high tensile strengths via precipitation hardening. These various crystal structures are controlled at any given temperature by alloying elements such as chromium, which stabilizes the ferrite phase, and nickel, which stabilizes the austenite phase. In fact, other alloying elements also contribute to stabilization of the austenite or ferrite phases. For example, the ferrite phase is stabilized by not only Cr, but also by Mo, Si, Nb, Ti, Al, V, and W. Similarly, the austenite phase is stabilized by Ni, Mn, C, N, Cu and Co. For ease of interpretation, these properties are combined into the notion of the "equivalent chromium" and "equivalent nickel" contents). (Table 2-1 and Eq. 2-1 and Eq. 2-2).

Eq. 2-1: $$Cr_{equiv} = (wt\%\ Cr) + F_{Si}\,(wt\%Si) + F_{Mo}(wt\%Mo) + \ldots$$

Eq. 2-2: $$Ni_{equiv} = (wt\%Ni) + A_{Mn}\,(wt\%(Mn) + A_{C}\,(wt\%C) + A_{N}\,(wt\%N) + \ldots$$

[2] Note that the American Iron and Steel (AISI) nomenclature will be used in this report, albeit recognizing that essentially the same alloys can be described by other designations such as those in the Unified Numbering System (UNS), (which includes non-ferrous alloys), as well as designations used in other countries (e.g. DIN) or proprietary alloy names.

The equilibrium phases (austenite, ferrite, martensite or duplex (austenite plus ferrite)) that are stable for a variety of "equivalent chromium" and "equivalent nickel" may be predicted via diagrams such as the Schaeffler diagram (Figure 2-3a) that was initially drawn for welding purposes and is reasonably accurate for conventional 300-series austenitic stainless steels and their weld deposits. However, steel makers use different diagrams and expressions of Cr_{equiv} and Ni_{equiv} that take into account more alloying elements than those of Schaeffler, for example those given by Harries [Harries, 1982] or those of Pryce and Andrews [Pryce & Andrews, 1960] (Table 2-1 and Figure 2-3b). The latter were used in France in the 70s and 80s to obtain Type 304 and 316 grades with very low ferrite content for primary circuit materials.

In addition, the formulations in Eq. 2-1 and Eq. 2-2 have limitations for predicting the ferrite content in duplex stainless steels with high nitrogen contents and with complex compositions. Thus, the formulations of Table 2-1 have been modified for some steels; these will be discussed further in Section 2.2.

Table 2-1: Coefficents of Eq. 2-1 and Eq. 2-2 for Ni_{equiv} and Cr_{equiv} in stainless steels according to different authors.

A_{el}	Shaeffler	Harries	Pryce & Andrews	F_{el}	Shaeffler	Harries	Pryce & Andrews	
							Mo < 1 wt%	Mo > 2 wt%
Co	--	1.0	--	Si	1.5	2.0	3.0	3.0
Mn	0.5	0.5	0.5	Mo	0.5	1.5	1.0	1.0
C	30	30	21	Al		5.5	--	--
N	--	25	11.5	Nb	--	1.75	--	--
Cu	--	0.3	--	Ti	--	1.5	--	--
				W	--	0.75	--	--

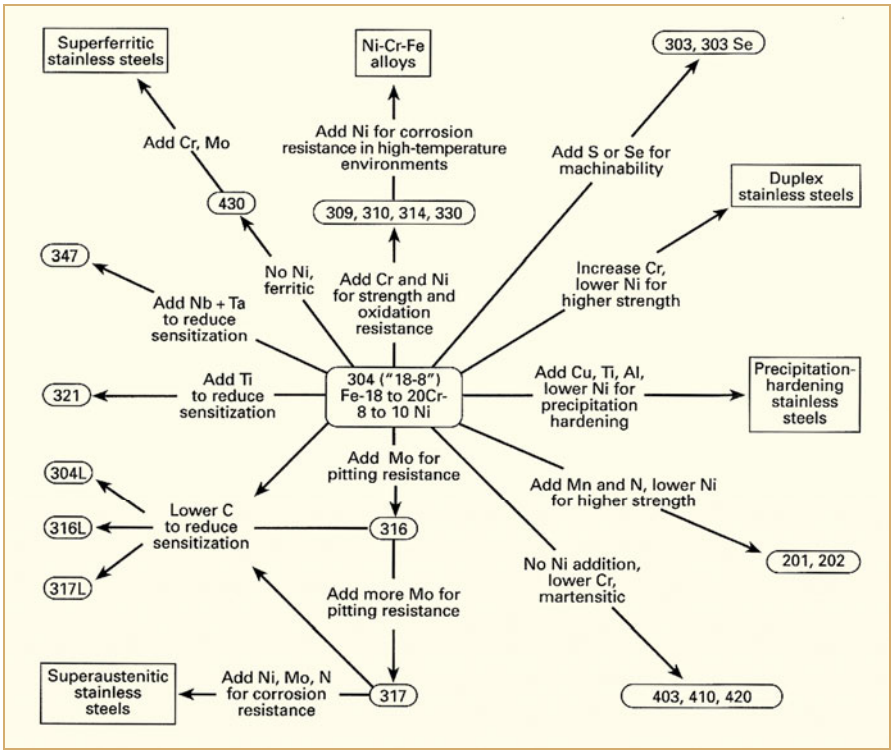

Figure 2-2: Compositional and property linkages in the stainless steel family of alloys [Sedriks, 1979].

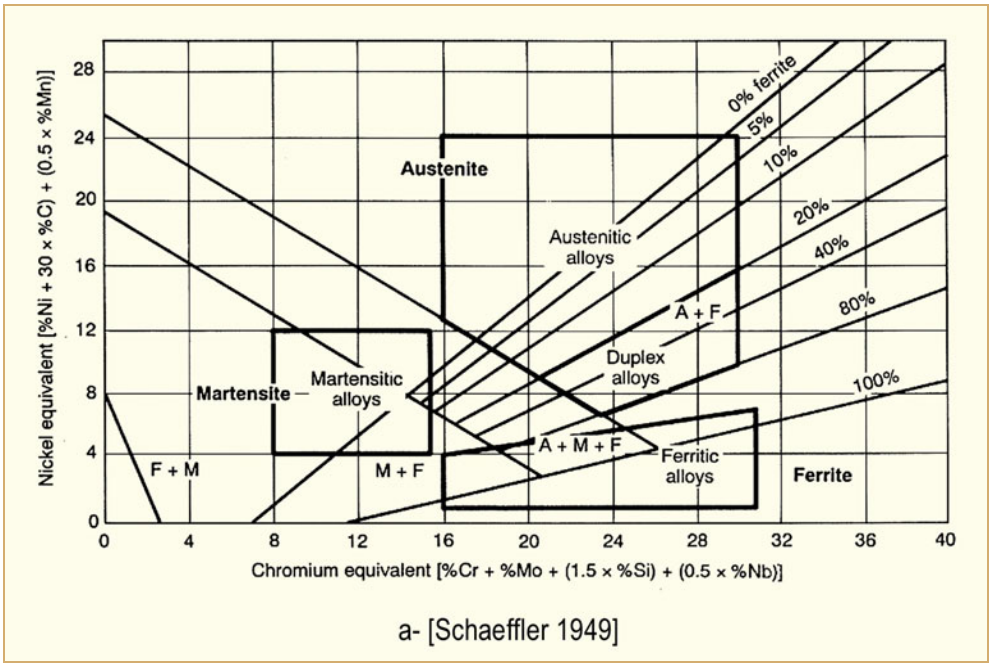

a- [Schaeffler 1949]

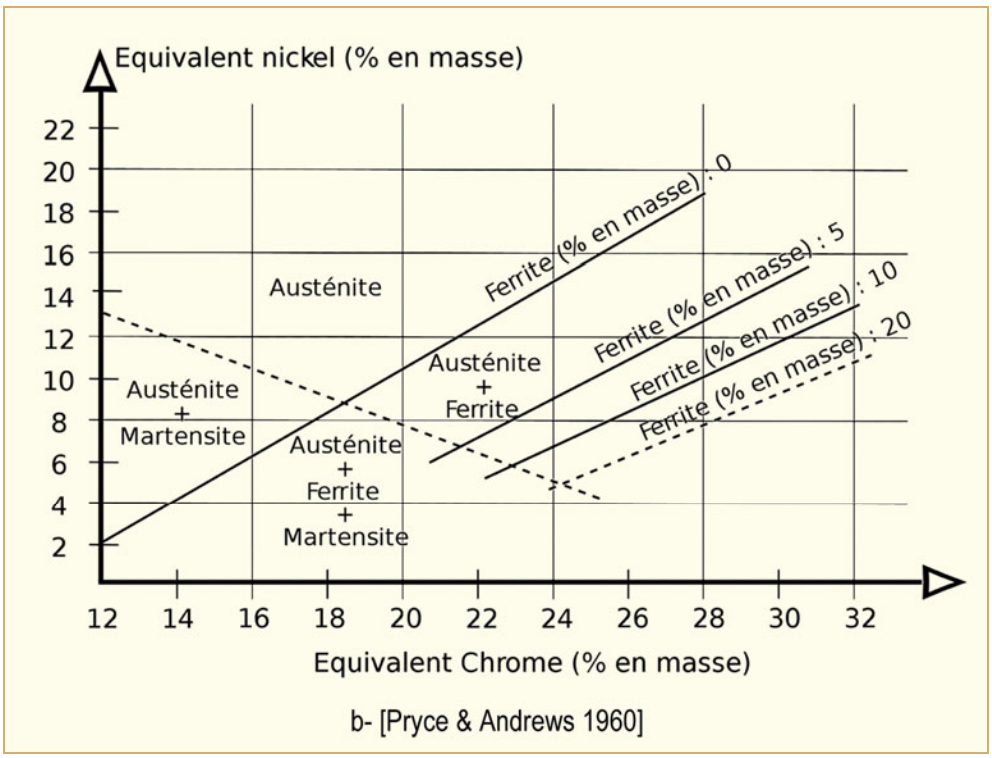

b- [Pryce & Andrews 1960]

Figure 2-3: Constitution diagram for stainless steels (a) [Schaeffler, 1949] (b) [Pryce & Andrews, 1960].

2.1 Austenitic stainless steels

The austenitic stainless steels (Table 2-2) based on the Fe-18Cr -10 Ni -0.03C median composition represents the largest category of stainless steel used in LWR primary systems. These steels have a face centred cubic (fcc) crystal structure due to the relatively high contents of elements such as nickel, manganese, carbon and nitrogen, which stabilize the austenite phase. Due to the number of slip systems in the fcc lattice, these austenitic structures are very ductile. It is seen in Figure 2-3, however, that the ductile austenite phase is metastable at the higher chromium–equivalent and lower nickel-equivalent compositions due to the formation of a second phase, ferrite, which has a body-centred cubic (bcc) crystal structure.

The austenitic fcc structure is easily fabricated and has good fracture resistance in air (when not subjected to high neutron fluence). Strengthening mechanisms are restricted to work hardening, (usually by cold working) or by precipitation hardening. As will be discussed later, however, the usefulness of cold working as a strengthening mechanism is limited due to a negative impact on SCC.

Excellent general corrosion resistance[3] is achieved via chromium contents in the range 16-20%. Other alloying elements include Mo, Cu, Al, Ti and Nb, which improve, for instance, localized corrosion resistance (e.g. the addition of Mo to minimize pitting) in chloride contaminated environments, or sensitization resistance (e.g. the addition of Ti or Nb in the "stabilized stainless steels").

Table 2-2: Compositions of wrought austenitic stainless steels used in US and German LWRs[4] [5].

AISI #	C	Mn	Si	Cr	Ni	P	S	N	Mo	Cu	Other
304	0.08	2.0	1.0	18-20	8-10.5	0.045	0.03				
304L	0.03	2.0	1.0	18-20	8-12	0.045	0.03				
304NG	0.02	2.0	0.75	18-20	8-11	0.03	0.005	0.06-0.1		0.5	(2)
316	0.08	2.0	1.0	16-18	10-14	0.045	0.03		2.0-3.0		
316L	0.03	2.0	1.0	16-18	10-14	0.045	0.03		2.0-3.0		
316NG	0.02	2.0	0.75	16-18	11-14	0.03	0.005	0.06-0.1	2.0-3.0		(2)
321	0.08	2.0	1.0	17-19	9-12	0.03	0.03				(3)
347	0.08	2.0	1.0	17-19	9-13	0.045	0.03				(4)
347NG	0.03	2.0	1.0	17-19	9-12	0.035	0.02				(5)

Notes:
1 - All compositions are maximum allowable unless a range is indicated
2 - Co 0.25 max., (Ta + Nb) 0.05 max., B 0.001 max., Al 0.04 max., V 0.1 max., (Bi+Sn + As + Sb + Se) 0.02max.
3 - Ti > 5 X C
4 - (Nb+Ta) > 10 XC
5 - 0.2Co, Nb > 10 X C

[3] See Chapter 3.
[4] Note that French specifications for stainless steels in LWR primary circuit are different from those in the table, generally with more restricted composition ranges to ensure resistance to sensitisation and very low ferrite content.
[5] Note that in German plants the 1998 KTA specification for the Type 347NG steel is tightened for those components operating at temperatures >200C to Si<0.5%, P< 0.025%, S<0.01%, 18%<%Cr<19%, and 13x(%C)<%Nb<0.65.

All of the austenitic stainless steels are susceptible to a phenomenon known as "grain boundary sensitization" which occurs when heated (usually during fabrication) in the temperature range approximately 550 to 850 °C (1000 to 1550 °F). This phenomenon is understood in terms of the equilibrium relationships shown in Figure 2-4 between the austenite matrix and carbide precipitates in an 18Cr-10Ni alloy. This simplified phase diagram indicates that carbon will remain in solid solution over the temperature range shown provided the carbon content is less than approximately 0.03 wt.%. At equilibrium, carbon in excess of 0.03 wt.% will precipitate as chromium-rich carbide, $(Cr_3Fe)_{23}C_6$ (or generically $M_{23}C_6$) at temperatures lower than the indicated solubility line.

This precipitation of $M_{23}C_6$ occurs (in decreasing order of preference) at high energy regions such as ferrite–austenite phase boundaries (if they exist), austenite grain boundaries, incoherent twin boundaries and, finally, at coherent twin boundaries [Stickler & Vinckier, 1961].

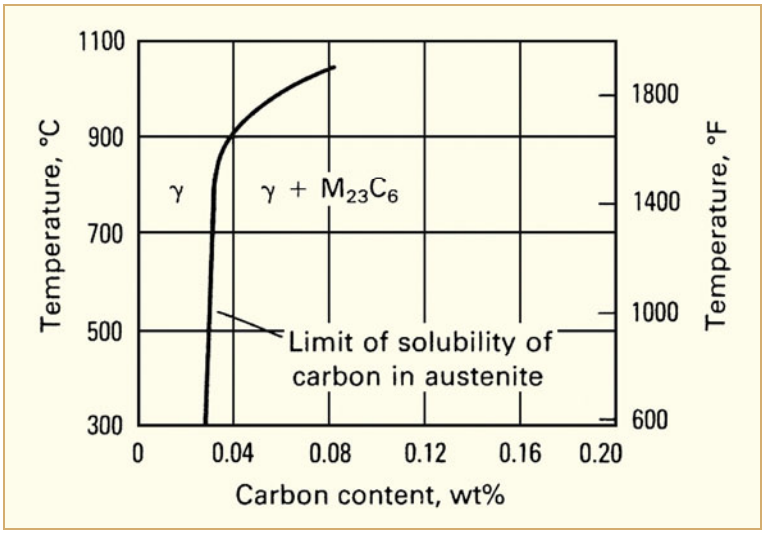

Figure 2-4: Solid solubility of carbon in an Fe-18Cr-8Ni alloy, indicating the equilibrium austenite (γ) and carbide phases [Husen & Samans, 1969].

The amount of $M_{23}C_6$ that precipitates at, for example, a grain boundary depends critically on the temperature and time combinations experienced during heating in the critical range. Lowering the temperature below the equilibrium temperature shown in Figure 2-4, (e.g. 900 °C for a 0.04% C steel) will increase the carbide *nucleation* rate. However, this lowering of the temperature will also decrease the subsequent rate of carbide *growth*, since lowering the temperature will decrease the diffusion rates of chromium and carbon atoms from the grain matrix to the grain boundaries where the carbide nuclei reside. The result of these competing effects of temperature on carbide nucleation and growth is shown in the Temperature-Time-Transformation (TTT) diagram shown in Figure 2-5 for austenitic 18Cr-8Ni steels containing different carbon contents. It is apparent that this precipitation reaction may be largely suppressed at relatively rapid rates of cooling from an austenitizing temperature above 900 °C. In this case, the room temperature microstructure is characterized by a single phase austenite supersaturated with carbon. However, if this supersaturated austenite is reheated to elevated temperatures[6] within the $(\gamma + M_{23}C_6)$ field, then precipitation and growth of the chromium-rich $M_{23}C_6$ will take place preferentially at the austenite grain boundaries.

[6] For example, a heat treatment at 600-650 °C for 1 to 4 hours for stress relief of nearby carbon and low alloy steel structures, such as pressure vessel nozzles. From Figure 2-5 it is seen that such a heat treatment will give $Cr_{23}C_6$ precipitation in an austenitic stainless steel containing 0.06%C.

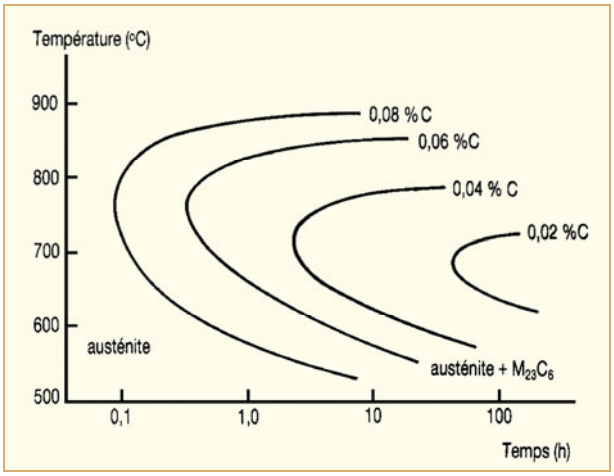

Figure 2-5: Time-temperature-transformation characteristics for 18Cr-8Ni stainless steels where $Cr_{23}C_6$ forms to the right of the line corresponding to the carbon content in the steel.

Chromium-rich carbides nucleate preferentially in high energy grain boundaries and, as they grow, there is an associated chromium depletion in the adjacent grain matrix when the time-temperature combinations are insufficient to diffuse the larger chromium atoms within the grain matrix into the austenite near to the growing grain boundary carbide. The result is the formation of envelopes of chromium-depleted austenite around the carbides (Figure 2-6a), which, because of the high diffusivity of the carbon along the grain boundary, may appear continuous even though the carbides are discrete. This grain boundary chromium depletion, called "sensitisation", occurs at short heat treatment times (0.5-10 hours at 7000C in the example shown in Figure 2-6b). However, as the heat treatment time increases, so the minimum grain boundary chromium increases, since the chromium from the grain matrix now has sufficient time to diffuse to the grain boundary. This process is known as "sensitisation healing" and can occur (after 24-100 hours in the example in Figure 2-6b). Time-temperature combinations leading to sensitisation of austenitic stainless steels are usually summarised in t Temperature Time Sensitization (TTS) diagrams (Figure 2-7) showing how elevated carbon content lead to sensitisation for shorter time and wider temperature ranges than low carbon contents.

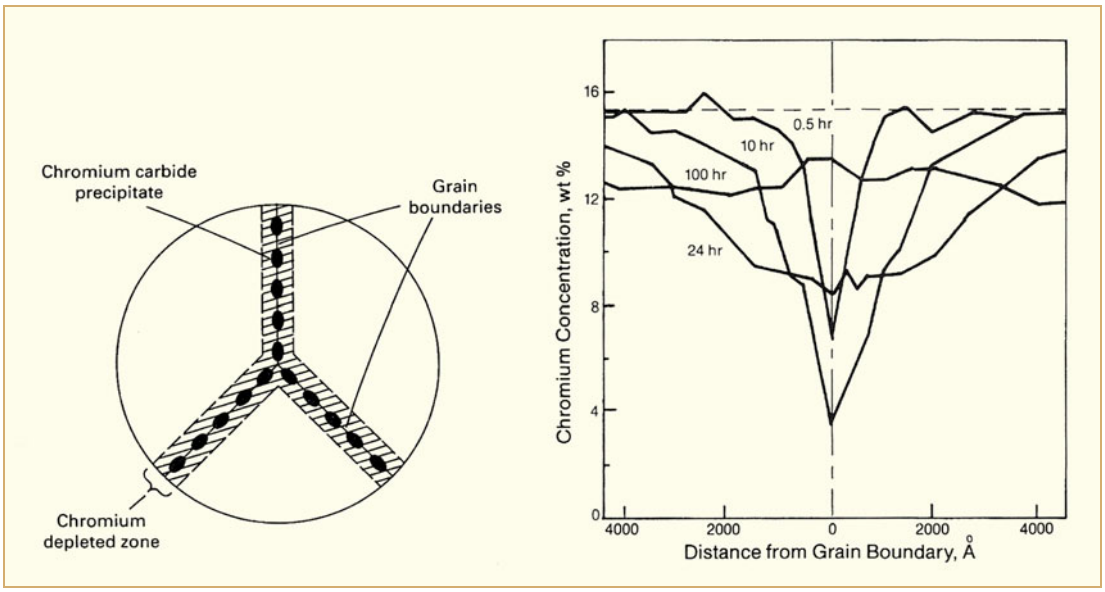

Figure 2-6: (a) Schematic representation of a sensitized grain boundary, (b) Chromium depletion associated with $Cr_{23}C_6$ precipitation following various aging times at 700 °C.

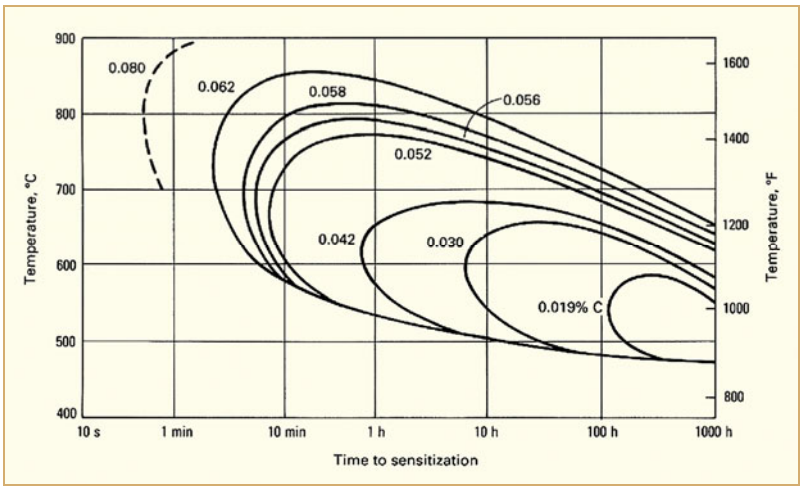

Figure 2-7: Time-temperature-sensitisation characteristics for 18Cr-8Ni stainless steels where $Cr_{23}C_6$ forms to the right of the line corresponding to the carbon content in the steel [ASM, 1994].

It is not surprising that this localized chromium depletion adjacent to grain boundaries can lead to intergranular corrosion attack or intergranular SCC in certain environments. This is discussed in more detail in Chapter 4 with emphasis on the prediction of material sensitization effects associated with different fabrication methods, stress and strain profiles, and operational environments (e.g. neutron irradiation-induced sensitization as compared with the thermal effects mentioned above; see Section 2.7). At this point, however, it is sufficient to point out that intergranular attack and, as illustrated in Figure 2-8, IGSCC is very sensitive to the minimum grain boundary chromium content that results from this thermally induced carbide nucleation and growth process. Indeed, the extent of chromium depletion may be characterized in terms of the amount of intergranular attack that occurs in a number of non-destructive electrochemical tests [Clarke et al, 1978] and [Clarke, 1980]. This point will be returned to later since a commonly used parameter, Electrode Potential Reactivation (EPR) to quantify the extent of chromium depletion, arises from such electrochemical tests.

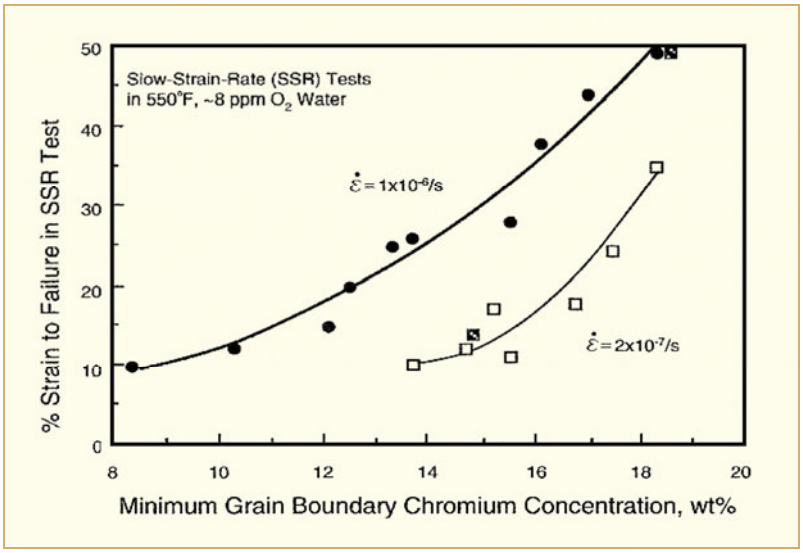

Figure 2-8: Influence of grain boundary chromium content on the % strain to failure during a Slow Strain Rate Test (SSRT) on sensitized stainless steel in oxygenated 288 °C water. Note that less than a 1% drop in Cr content adjacent to the grain boundary from the nominal 18% in the bulk material can have a significant effect on the IGSCC susceptibility. The two curves are associated with the two applied strain rates used in the slow strain rate SCC test [Bruemmer et al, 1993].

In addition to the temperature/time/carbon content combinations that may affect the susceptibility of the stainless steels to grain boundary sensitization, other metallurgical factors [Briant, 1982] may have an effect. Increasing nitrogen[7] and molybdenum alloying additions retard the sensitization rate, while cold work, (as will be discussed in Chapters 4 and 5), [Bose & De, 1987], accelerates the sensitization rate since the chromium diffusion rates are increased by the dislocation structure resulting from cold work.

The temperature-time combinations that lead to chromium depletion adjacent to grain boundaries may be achieved by the cumulative heat inputs associated with multi-pass welding in the "Heat Affected Zone" (HAZ) of the adjacent parent metal. The resulting environmental attack has been described as "weld decay". The temperature-time combinations may also be met during the stress relief furnace heat treatments for attached carbon and low alloy steel structures; in this case, the phenomenon has been classified as "furnace sensitization". Another nomenclature that has been used is "Low Temperature Sensitization (LTS)", which refers to the possibility that the growth of pre-nucleated grain boundary $M_{23}C_6$ and hence the chromium depleted zone, may occur over very extended times at temperatures as low as 288 °C. This would raise the possibility that sensitization may occur during reactor operations in addition to that arising during fabrication. Certainly this may occur to some extent, as shown in Figure 2-9 by the 1/T vs. sensitization time relationship that forms the boundary between "cracking" and "no cracking" in both constant load and SSRTs in oxygenated high temperature water. However, it is apparent that because of the bimodal relationship in Figure 2-9, long operational times (30 years) at temperatures ~300 °C would be required in order to sustain IGSCC. It follows that such a phenomenon could be of potential concern for extended life operation of 60-80 years.

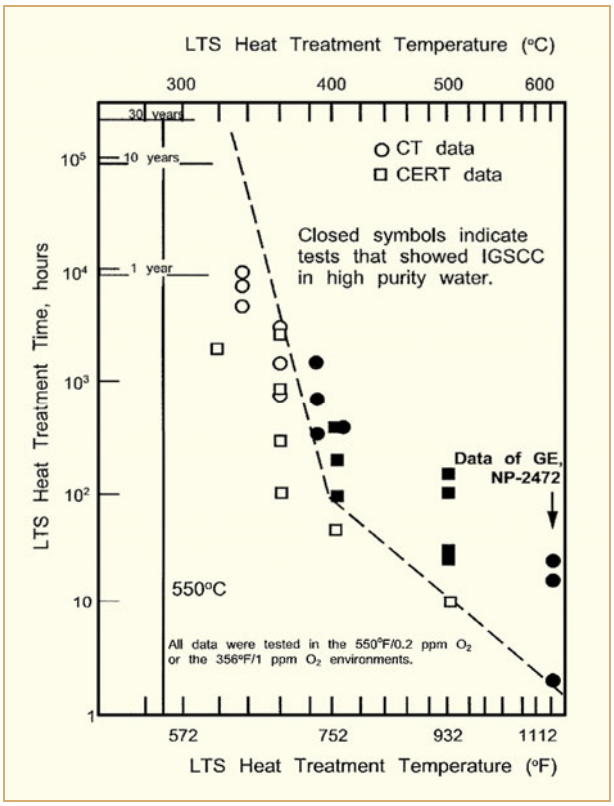

Figure 2-9: Temperature/ time sensitizing combinations required to give IGSCC in stainless steel in oxygenated water at 288 °C. Filled points denote that cracking was observed in two test procedures: slow applied strain rate (Constant Extension Rate Test (CERT)) and constant load pre-cracked (Compact Tension (CT)) tests.

[7] Note, however that very high nitrogen contents can give rise to sensitization due to the formation of chromium carbides.

The position of the crack in the HAZ relative to the Weld Fusion Line (WFL) is governed by the material composition and heat input (which maximize the degree of grain boundary chromium depletion), and the weld joint design including total heat input during welding and stress relief (which determine the tensile residual stress). In earlier piping systems, for example, where high carbon content stainless steels were common (e.g. > 0.05%), intergranular cracks were typically located approximately 5 mm from the WFL. However, with the use of lower carbon L-grade stainless steels and refined welding practices, such as narrow gap Gas Tungsten Arc Welding (GTAW), fine-line and electron beam welding techniques with low heat inputs, the corresponding distance between the crack location and the fusion line is considerably less, and is governed primarily by the strain gradient immediately adjacent to the WFL. This point will be addressed later when discussing the effect of strain localization on the cracking susceptibility of unsensitized stainless steels in Section 4.5.4.

From a life prediction viewpoint, it is important that such sensitization phenomena are predictable. This has been the objective of extensive investigations over many decades with the focus on predicting the depleted chromium profile adjacent to grain boundaries as a function of alloy composition, cold work, isothermal temperature/time combinations, and welding history (such as, heat input, component size, number of weld passes, etc.) [Solomon & Lord, 1980], [Solomon, 1980], [Solomon, 1984], [Bruemmer, 1988], [Bruemmer et al, 1988a] and [Bruemmer et al, 1988b]. An example of such a comparison between theory and observation is shown in Figure 2-10 for the variation of the EPR value (as a measure of sensitization) on the inside diameter of a welded pipe as a function of the carbon content of the stainless steel and the number of weld passes.

Grain boundary chromium depletion may also occur in the grain boundary without the $M_{23}C_6$ precipitation, which is governed by the thermal equilibrium arguments given above. It occurs as a result of neutron irradiation; the physics of this has also been the object of intense analysis; see Section 2.7 and [Andresen et al, 1990a], [Andresen & Ford, 1995], [Nelson & Andresen, 1992] and [Bruemmer et al, 1996]. In this case, chromium depletion, together with irradiation-induced metalloid segregation also reduces IGSCC resistance and may be additive to that associated solely with thermal sensitization. This topic is discussed in more detail in Sections 2.7.1 and 4.6 covering irradiation effects on microstructure and SCC.

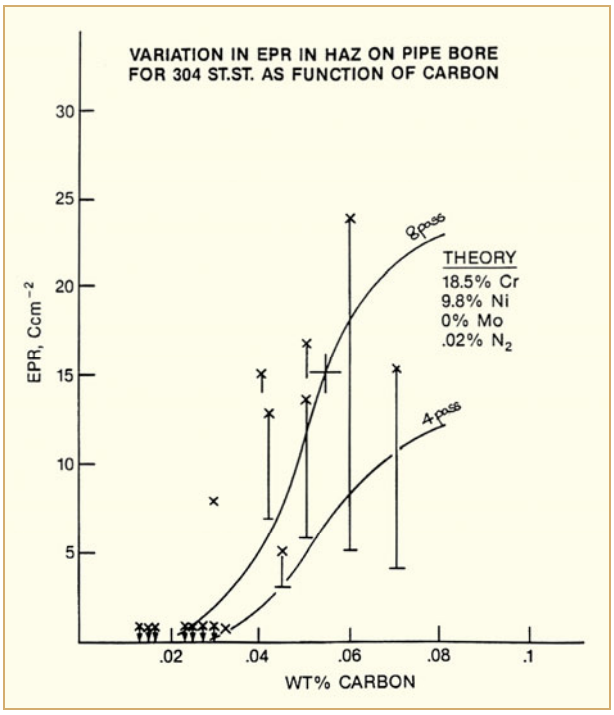

Figure 2-10: Observed and theoretical variations in EPR values in the HAZ adjacent to the weld on the bore of 4" diameter Type 304 stainless steel piping as a function of the carbon content in the parent material and the number of weld passes [Ford & Andresen, unpublished data, 1997].

Control of thermally-induced grain boundary sensitization has been the driver in the development of fabrication control techniques and of different SCC resistant grades of austenitic stainless steel in Table 2-2. For example, the degree of sensitization may be decreased by:

a) Controlling the heat input to the structure during fabrication, i.e. avoiding the "nose" in the TTS diagram. This may be accomplished by different welding practices as well has control of stress relief heat treatments.

b) Decreasing the carbon content (as in the L-grade 3XX steels) as indicated by the different TTS relationships in Figure 2-7. Such a change in composition can lead to a drop in yield and tensile strength, but this may be counteracted by the addition of nitrogen (i.e. the NG – grade 3XX steels).

c) Annealing the material prior to welding to remove the effect of cold work, which may accelerate the sensitization process.

d) Decreasing the heat input or heat extraction rates during welding by using low weld heat inputs and low interpass temperatures, and/or by water cooling the inside of pipes after the initial weld root pass.

e) Adding other strong carbide formers that combine with carbon preferentially rather than chromium. Such alternative carbide formers form the basis of the stabilized stainless steels and include niobium (Type 347 stainless steel) and titanium (Type 321 stainless steel) alloying additions. The use of these stabilized stainless steels has been extremely effective in mitigating localized corrosion phenomena, but it does require strict control over not only the temperature-time combinations that avoid $Cr_{23}C_6$ precipitation, and also the kinetics of precipitation and dissolution of the TiC or NbC phases that occur at ~1200 °C (Figure 2-11). This latter aspect is particularly important since the TiC and NbC carbides dissolve at temperatures > 1300 °C. In this case, chromium-rich $M_{23}C_6$ carbides can precipitate very close to the WFL and then lead to "knifeline" intergranular attack and SCC.

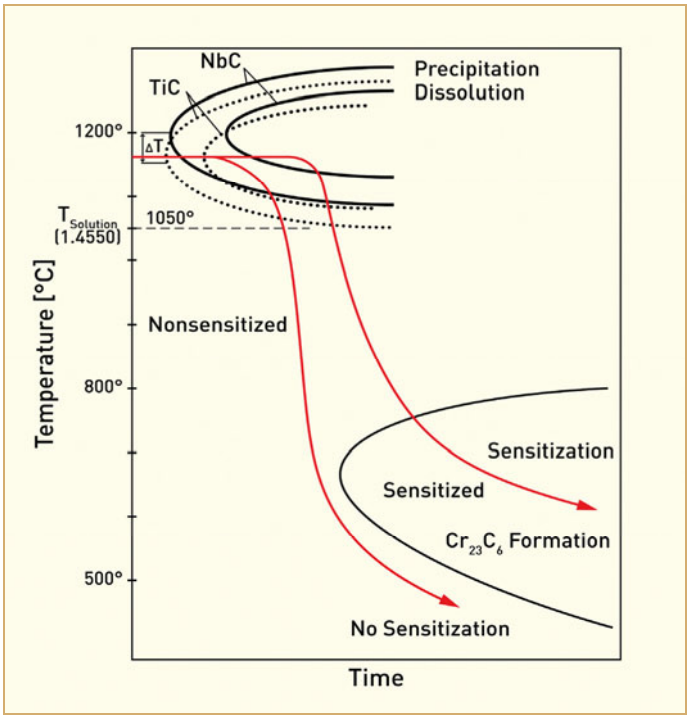

Figure 2-11: TTT diagrams for TiC and NbC precipitation and dissolution, illustrating the necessity for controlling the high temperature heat treatment in order to avoid $Cr_{23}C_6$ grain boundary precipitation and sensitization at the lower temperature [Ilg, 2008].

2.2 Duplex stainless steels, welds and cladding

Duplex stainless steels such as Type 308 and 308L (Table 2-3) are used as weld filler metals for joining of wrought austenitic stainless steel components by gas tungsten arc (GTA), Shielded Metal Arc Welding (SMAW) or Submerged Metal Arc (SAW) welding procedures. Type 309 and 310 duplex stainless steels are also used in some cases for dissimilar metal joints such as between Type 304 stainless steel piping and low alloy steels as the first butter layer applied to the low alloy steel component. These duplex stainless steels are also widely used as cladding materials on all carbon and low alloy steel surfaces exposed to the reactor coolant in order to minimize radioactive Chalk River Unidentified Deposits (CRUD) formation that would otherwise form due to general corrosion of low alloy steels[8]. The higher chromium content Type 309 alloy is used as the first layer of cladding or welding on low alloy steels since this counters the effect of chromium dilution at the weld fusion boundary.

Table 2-3: Nominal compositions of duplex and Cast Stainless Steels (CASS).

AISI #	C	Mn	Si	Cr	Ni	P	S	N	Mo	Cu	Other
Duplex Stainless Steels											
308	0.08	1.0-2.5	0.3-0.65	19.5-22	9-11	0.03	0.03		0.75	0.75	
308L	0.03	1.0-2.5	0.3=0.65	19.5-22	9-11	0.03	0.03		0.75	0.75	
309	0.12	1.0-2.5	0.3-0.65	23-25	12-14	0.03	0.03	0.6-0.10	0.75	0.75	
310	0.08-0.15	1.0-2.5	0.3-0.65	25-28	20-22.5	0.03	0.03	0.6-0.10	0.75	0.75	
Cast Stainless Steels											
CF8	0.08	1.5	2	18-21	8-11	0.04	0.04		0.5		
CF8M	0.08	1.5	1.5	18-31	9-12	0.04	0.04		2.0-3.0		
CF3	0.03	1.5	2.0	17-21	8-12	0.04	0.04		0.5		
CF3M	0.03	1.5	1.5	17-21	9-13	0.04	0.04		2.0-3.0		
All compositions are maximum allowable unless a range is indicated											

The main issues in choosing a cladding or weld filler metal are, first that it has adequate general corrosion resistance in the reactor coolant, second that it is compatible with the parent material[9] and, third it is resistant to the formation of defects either during or after the welding/cladding operation. The first of these criteria is largely met by the high chromium content in the stainless steel family.

Consequently, satisfying the second and third criteria becomes paramount, which is dependent on countering the formation of a variety of weld defects including hot cracks, (which occurs during the welding process at temperatures just below the solidus temperature), and cold cracking that occurs during or immediately after the welding process. Hot cracking is more commonly found in austenitic alloys, while the latter is often observed in the higher strength martensitic and (precipitation hardening) PH stainless steels, and in ferritic stainless steels where the weldments have become embrittled by grain coarsening and second phase precipitation. Cold cracking is usually associated with hydrogen embrittlement, where the hydrogen often comes from moisture present during welding. This will be discussed later in Section 2.6.1.

[8] Note that the general corrosion rate for carbon and low alloy steels in LWR environments is low in high temperature water due to the formation of a protective magnetite/haematite surface layer. However, there is no question that a stainless steel cladding is beneficial to avoid corrosion and pitting of the low alloy steels at lower temperatures associated with reactor shut down/startup and layup.

[9] In terms of coefficient of thermal expansion, for example, since this will have an effect on thermal stresses during welding.

Hot cracking may be counteracted by ensuring that > 3% ferrite is present in the solidifying weld, and that this phase forms first during the solidification process. Of perhaps secondary importance is the control of low melting point liquid phases associated with impurities such as P, S, B, Se, Si, and Nb; Mn additions can be beneficial in this regard since they tie up S and Si impurities.

As discussed earlier, the presence of ferrite in the weld metal is dependent on the relative values of Cr_{equiv} and Ni_{equiv} and the validity of the formulations (Eq. 2-1 and Eq. 2-2) for these parameters.

As indicated in Figure 2-3, mixtures of austenite and ferrite phases are stable for those alloys that have higher chromium-equivalent and lower nickel-equivalent compositions than the austenitic stainless steels. However, it should be noted that the Schaeffler diagram (Figure 2-3a) may give erroneous estimates of the ferrite content for complex alloys. Consequently, there have been several modifications proposed for the Cr_{equ} and Ni_{equ} formulations [Kaltenhauser, 1971], [Long & Delong, 1973], [Delong, 1974], [Siewert et al, 1988] and [Kotecki & Siewert, 1992].

Delong recognized [Delong, 1974] that the Schaeffler formulation for Ni_{equiv} did not adequately account for the effect of the elevated nitrogen contents in Types 309, 316 and 310 stainless steel and, therefore, modified the formulation for this parameter as follows;

Eq. 2-3: $$Ni_{equiv} = Ni + (30 \times C) + (30 \times N) + (0.5 \times Mn)$$

The Delong formulations were subsequently found to overestimate ferrite contents in higher alloyed duplex stainless steels. Consequently, the Welding Research Council (WRC) developed alternative formulations in 1988 [Siewert et al, 1988] and then with further modifications (Eq. 2-4 and Eq. 2-5) in 1992 [Kotecki & Siewert, 1992]:

Eq. 2-4: $$Cr_{equiv} = Cr + Mo + 0.7Nb$$

Eq. 2-5: $$Ni_{equiv} = Ni + (35 \times C) + (20 \times N) + 0.25Cu$$

A further advantage of the WRC formulations was that they included the Cr_{equiv} and Ni_{equiv} combinations that governed whether the austenite or ferrite phases solidified first during welding operations. The importance of this latter criterion is illustrated in Figure 2-12, which indicates the beneficial effect of maintaining a (Cr_{equiv}/Ni_{equiv}) ratio >1.5 in order to minimize hot cracking, even in the presence of large amounts of P and S.

Grain boundary sensitization can occur at both the austenite/ Cr23C6 and the ferrite/Cr23C6 boundaries and this can give rise to SCC in oxygenated BWR environments. However, the degree of chromium depletion at the ferrite/Cr23C6 boundary is significantly reduced compared with that at austenite/Cr23C6 boundaries. This is because (a) Cr diffusion in the bcc ferrite phase is much faster than in the fcc austenite phase leading to much quicker “healing” of the chromium depletion profile at the ferrite/Cr23C6 boundaries, and (b) the chromium content in the ferrite phase is elevated to approximately 25% during the solidification process of welds or cladding. Thus, in general, SCC of duplex stainless steel weld metal and cladding in BWRs is relatively rare provided the ferrite content is > 7.5% (NRC 1978) and especially if low-carbon (L grade) compositions are adopted. However, there have been isolated instances of SCC, and these have usually been associated with either low ferrite contents, the application of post weld heat treatments that severely sensitized the structure, or impure oxidizing conditions in the BWR coolant.

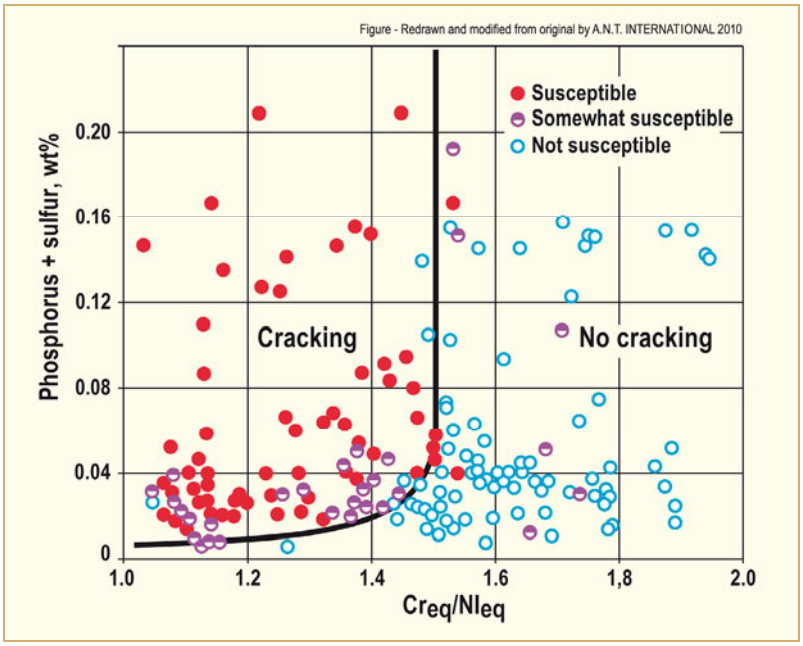

Figure 2-12: Relationship between solidification cracking susceptibility and Cr_{eq}/Ni_{eq} ratio. Boundary between cracking and no-cracking at ratios <1.5 corresponds to the austenite phase solidifying first while a ratio >1.5 corresponds to ferrite solidifying first [Takalo et al, 1979].

2.3 CASS

CASS (Table 2-3) are widely used in both BWRs and PWRs for pump and valve casings and in BWRs for reactor internals such as jet pump assemblies. Some PWR core support structures below the core itself may also be fabricated from CASS. These alloys have a duplex austenite /ferrite structure usually with approximately 10-15% ferrite and have similar mean compositions to the wrought stainless steels (Table 2-2), albeit with a wider composition range.

CASS alloys contain much higher ferrite than the wrought alloys in order to obtain good strength, good casting capability, and weldability. They have, therefore, slightly higher Cr and Si contents and lower Ni contents compared to the wrought alloys. The higher ferrite content plus the low carbon content in CF-3 and CF-3M alloys minimizes the danger of SCC in comparison to that in the wrought 3XX alloys.

Service experience mirrors this laboratory expectation since, in the few cases where SCC has been observed in BWR plant, it has been associated with heats that have a higher carbon content (CF8, CF8M), or have been sensitized and cold worked, and where the minimum 7.5% ferrite specification has not been met.

One area of potential concern is that CASS alloys are susceptible to thermal embrittlement at temperatures and times relevant to extended LWR service. The mechanism for such embrittlement is discussed in Section 2.6.1, but the issue is mentioned here since there is a reasonable possibility that such a reduction in fracture resistance due to compositional changes may well (but not yet demonstrated) have a synergistic effect on subcritical crack propagation rates due to SCC. In PWR service, the molybdenum modified grades have proved to be much more susceptible to thermal ageing.

2.4 High strength stainless steels

Various high strength alloys are used in both BWRs and PWRs as replaceable components such as valve stems, springs, jet pump beams and bolts. These alloys are based on low alloy steels (in containment environments), nickel-base alloys and stainless steels, where the hardening is associated with work hardening and/or precipitation and martensite formation. The focus in this section is confined to stainless steels (Table 2-4). The attendant danger of embrittlement that accompanies high strength conditions is addressed in Section 2.6.

Table 2-4: Nominal compositions of some high strength stainless steels.

AISI #	C	Mn	Si	Cr	Ni	P	S	N	Mo	Cu	Other
Martensitic Stainless Steel											
A410	0.15	1.0	1.0	11.5-13.5		0.04	0.03				
PH Austenitic Stainless Steel											
A286	0.08	2.0	1.0	13.5-16.0	24.0-27.0	0.025	0.025		1.0-1.5		(2)
PH Martensitic Stainless Steel											
17-4 PH	0.07	1.0	1.0	15.0-17.5	3.0-5.0	0.04	0.03				(3)

Notes: 1 - All compositions are maximum allowable unless a range is indicated
2 - 1.9-2.3 Ti, 0.1-0.5 V, 0.01B
3 - 3.0-5.0 Cu; 0.15-0.45 Nb

Wrought austenitic stainless steels (Table 2-2) in the annealed condition have modest tensile properties with yield strength 205-275 MPa (30 - 40 ksi), ultimate tensile strength 520-760 MPa (75-100 ksi), and tensile elongations of 40 - 60%. These alloys can however be significantly work hardened by cold work, with a correspondingly high ultimate tensile stress of 1200 MPa (175 ksi) or even higher. However, deliberate strain hardening for stainless steel components exposed to LWR coolants should be limited to a maximum yield strength of 90 ksi (or 625 MPa) [USNRC, 2005], as specified for material for core support structures that is susceptible to SCC (Code case N-60-5) and discussed in Reg. Guide 1.85.

These increases in yield strength either by design or due to inadvertent abuse (usually of the surface) during fabrication, have had a significant effect on the SCC susceptibility of wrought Type 3XX alloys, and this specific effect will be discussed in detail in Section 4.5.4. Observations of the effect of cold work on SCC were initially made for BWR components operating in relatively oxidizing environments and, as a result, in General Electric (GE) BWRs the amount of strain hardening is confined to < 5%, This allowable strain hardening range is expanded to 5-15% in titanium modified Type 316 stainless steels used for reactor internals in German BWRs. In this case, the cracking susceptibility was minimized since this particular steel was used in the duplex microstructural condition with Ti additions to minimize any possible thermal sensitization (due to $M_{23}C_6$ formation). The use of cold worked wrought Type 3XX stainless steel components is more widely allowed for PWR components (cold bent piping, reactor internals, bolting) where the environment is less oxidizing.

Alternatively, Alloy XM-19, a wrought 20-23% Cr, 11-14% Ni, alloy containing 0.2-0.4% N for strengthening purposes has been widely used in the annealed condition in both BWRs (control rod drive components) and PWRs (reactor coolant pump shafts and bolting). No deleterious SCC has been observed to date since nitriding may be accomplished without grain boundary sensitization. These alloys may also be used in the hot or cold worked condition to give an ultimate tensile strength of 927MPa (135ksi) (and a yield strength ≤ 90ksi). However, caution is required since this steel has been only used in BWR applications in the cold or warm worked condition since the mid 1990's and there is insufficient experience to indicate if the good performance of the annealed condition is repeated.

Attention is now directed in this section to those compositional changes and heat treatments where the tensile strengths have been increased via (a), the formation of martensite in stainless steels, (b), precipitation hardening in martensitic stainless steels, and (c) precipitation hardening of austenitic stainless steels.

2.4.1 Martensitic stainless steels

The increased strengths of these steels derive from the presence of martensite, which forms via an athermal process upon cooling the austenite phase. Thus, the pre-existing presence of austenite is crucial.

Martensitic stainless steels have chromium contents in the range 10.5-18% and carbon contents as high as 1.2%, (although for the standard Type 410 steel, the carbon content is much lower at ≤0.15%). The chromium and carbon levels are balanced in order to stabilize the austenite phase at a temperature above 980 °C. As seen in the equilibrium iron/chromium phase diagram in Figure 2-13, an austenite structure is not stable beyond approximately 12% chromium for steels with low carbon and nitrogen contents. However, this stability region (or "austenite loop") is expanded with increasing carbon and nitrogen concentrations so that austenite is stable at 980 °C for the carbon contents specified for martensitic stainless steels such as Type 410 (see Table 2-4).

The isothermal TTT diagram for the formation of the stable phases below 980 °C is indicated in Figure 2-14a for a Type 410 stainless steel. It is seen that even a moderate cooling rate from this austenitization temperature will avoid the formation of ferrite and carbides, and will allow the athermal transformation of the "soft" austenite to a high hardness body-centred tetragonal martensite phase at a M_{start} [10]temperature of 350 °C. The resulting hardness can be high, and as indicated in Figure 2-13b, is markedly dependent on the carbon content. Further alloying elements such as Nb, Si, W and V may be added in order to further delay the precipitation of ferrite or alter the kinetics of subsequent hardening processes.

[10] M_{start} refers to the temperature when the athermal transformation to martensite starts. As indicated in Figure 2-14(a) other temperatures may be quoted, corresponding to different amounts of martensite that are formed (e.g. 50% or 90%).

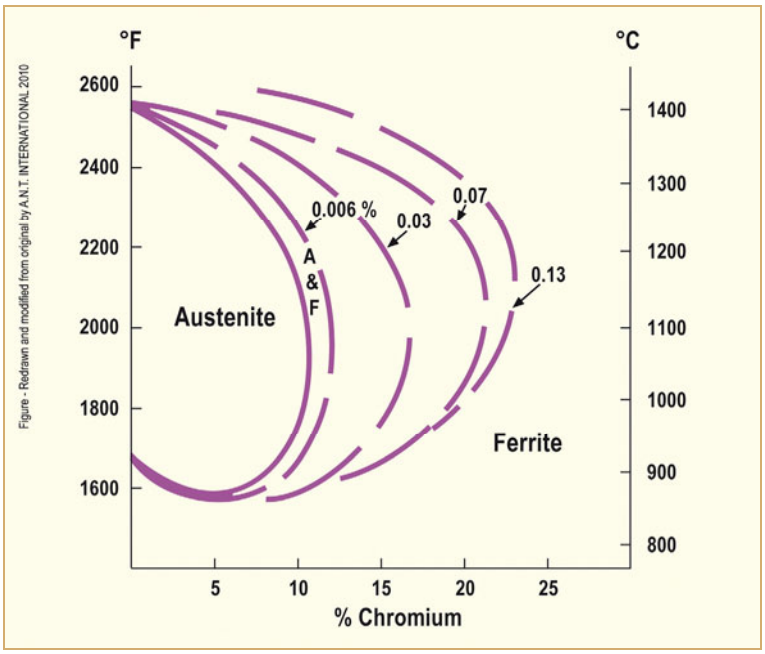

Figure 2-13: Effect of carbon and nitrogen (given equal weights) on increasing the stability of the austenite phase [Baelecken et al, 1961].

Welding difficulties can be encountered, however, due to delayed hydrogen cracking (see Section 2.6.1) but process control procedures are well defined.

As stated earlier, martensitic stainless steels are widely used in LWRs in components such as turbine blades, valve stems, pump shafts, etc. Their performance is generally satisfactory although they can be susceptible to SCC when heat treated to hardness levels >HR_C 26 (274VHN[11]). This susceptibility can be avoided by tempering the "as quenched" martensitic structure at temperatures circa 600-650 °C. Care is necessary in this process, however, since these alloys can suffer from temper embrittlement at temperatures in the range 400-450 °C.

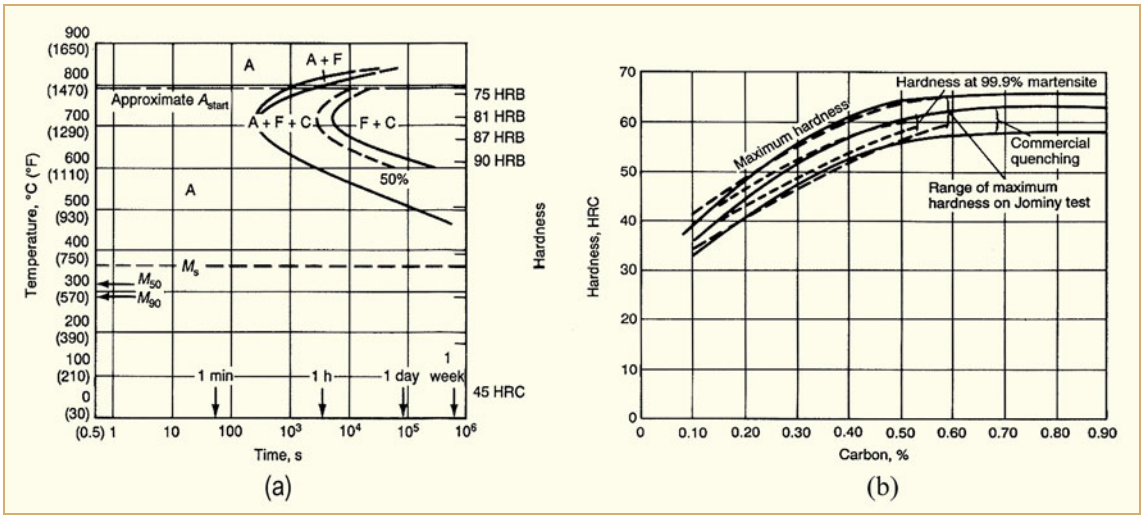

Figure 2-14: (a) TTT diagram for Type 410 stainless steel (12Cr 0.15%C) austenitized at 980 °C. (b) Hardness values (Rockwell C) of fully hardened martensitic stainless steel as function of carbon content [ASM, 1994].

[11] Vickers Hardness Number (VHN)

2.4.2 Precipitation hardening martensitic and austenitic stainless steels

The PH martensitic stainless steels, for which the 17-4 Precipitation Hardened (PH) grade (Table 2-4) is typical and is widely used, gain their high strength from martensite combined with precipitation hardening. The martensistic transformation is easily realizable by oil or air cooling from a solutionizing temperature of 1035 °C, which is then followed by a further aging heat treatment of 480 to 620 °C for 1 to 4 hours resulting in the formation of a strengthening face centred cubic Cu-rich phase. These steels have exhibited high SCC susceptibility particularly when the yield stress exceeds 1105MPa (170 ksi). Thus, it is recommended [Pathania, 2002] that these steels, which are used for, for example, replaceable items such as valve stems, pump shafts and bolting, are not used in the H900 condition but rather in the lower yield stress H1100 or H1150 conditions[12]. Further, long exposure times at reactor operating temperatures are not advisable since aging (and the resultant increase in yield stress) can lead to both a decrease in fracture toughness and an increase in SCC susceptibility, especially under oxidizing, impure localized environment conditions.

The PH austenitic stainless steel A-286 (Table 2-4), has a higher Ni content and a lower M_{start} temperature than the PH martensitic stainless steels, and consequently a martensitic structure cannot easily form by cooling from the solutionizing temperature of 900 °C. The hardening mechanism is provided by a subsequent aging treatment of typically 730 °C for 16 hours during which a γ' $Ni_3(Al,Ti)$ phase forms to provide precipitation hardening.

Alloy 286 is markedly sensitive to IGSCC at applied stress levels as low as 30% of the yield stress in BWR environments and 80% of the yield stress in PWR applications. For example, IGSCC was observed in A286 core grid screws [Bengtsson & Korhonen, 1983] in 1982 at the ASEA-ATOM BWRs at Forsmark -1 & 2 and TVO 1 & 2 plants after only 1-3 years of operation. The problem was extensive with 30% of the 500-700 screws in these plants being cracked. Its use in GE BWRs (operating under oxygenated water conditions) was been discontinued, and in PWRs there are severe controls on the stress (including stress concentration factors), as described in Section 5.3.

2.5 Ferritic stainless steels

Table 2-5: Nominal compositions of ferritic stainless steels.

AISI #	C	Mn	Si	Cr	Ni	P	S	N	Mo	Cu	Other
Ferritic Stainless Steels											
430	0.12			16-18							
405	0.08			11.5-14.5							0.1-0.3 Al
444	0.02	2		18	0.4			0.02	2		0.5 Ti
1. All compositions are maximum allowable unless a range is indicated											

[12] The numbers 900, 1100, 1150 refer to the aging temperature (°F), with a lower yield stress being associated with the higher aging temperature. Note also the in-service thermal ageing problems that have been encountered in PWRs described in Section 5.3.

Figure 2-3 indicates that the bcc ferrite phase is favoured as the nickel-equivalent content decreases and the chromium-equivalent increases. This is exploited for the ferritic stainless steel alloy family. The nominal compositions of three generations of ferritic stainless steels are illustrated in Table 2-5. In the first "standard" generation, epitomized by Type 430 stainless steel, the chromium content is greater than 16-18%, and the nickel content is minimal. As would be expected from the elevated chromium content, the general corrosion resistance is good. However, depletion of chromium at grain boundaries can occur due to the formation of grain boundary carbides when the chromium content is >15% [ASM, 1994] and intergranular corrosion is then possible. As noted in Figure 2-15, the formation of $Cr_{23}C_6$ carbides in ferritic stainless steels is faster than in the austenitic steels, which is attributable to the faster diffusion rate of the Cr in the ferritic matrix. As might be expected from the austenitic stainless steels, such sensitization may be counteracted by alloying additions of titanium and molybdenum and a reduction in carbon content (as, for example, in Type 444 stainless steel).

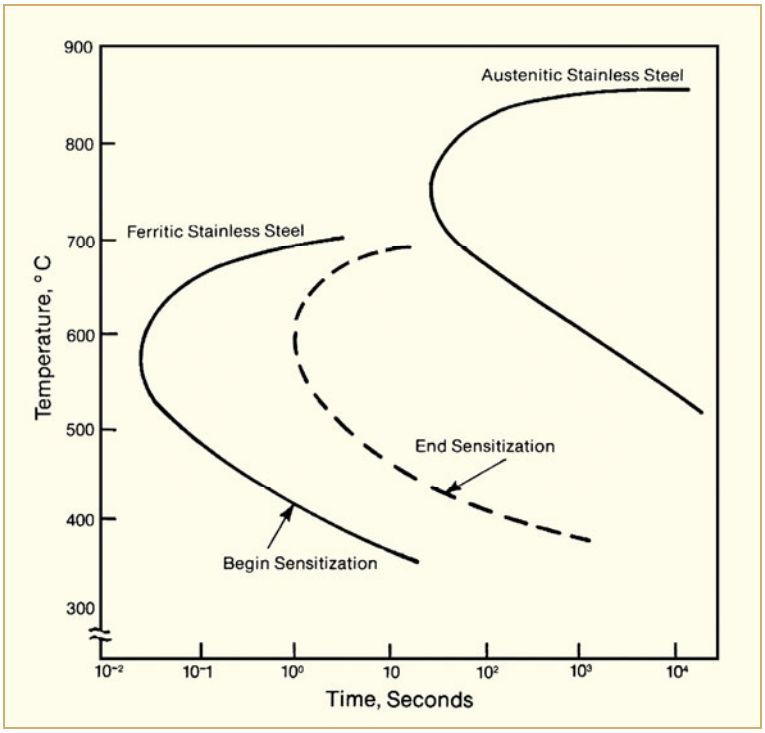

Figure 2-15: Temperature/Time/Transformation (TTT) relationships for the grain boundary precipitation of $Cr_{23}C_6$ in ferritic (Fe-Cr) and austenitic (Fe-Cr-Ni) stainless steels [Cowan & Tedman, 1973].

The initial attraction of these ferritic stainless alloys was their good general corrosion resistance and, unlike the austenitic stainless steels, their high resistance to SCC in chloride-containing environments. These alloys are not, however, widely used for passive components in LWRs for a variety of reasons including:

a) Localized corrosion of the weld metal unless there is control of the carbon and nitrogen contents in concert with the chromium content [Demo, 1974]. In addition, the presence of martensite in the weld metal can accelerate localized corrosion, especially if the chromium content is low, and it may also lead to decreased fracture toughness. The concern for the presence of martensite in the weld metal has led to the development of a modified Schaeffler diagram that predicts the combinations of ferrite and martensite as a function of the Cr_{equiv} and Ni_{equiv} parameters for weld metals (Figure 2-16).

b) An increased propensity for embrittlement, which is associated with the formation of σ phase at elevated temperatures (800 °C) and other phases at lower temperatures (e.g. "475 °C embrittlement"). These embrittlement mechanisms are discussed in Section 2.6.1.

3 Corrosion basics of stainless steels (Peter Scott, Peter Ford and Pierre Combrade)

3.1 Corrosion potential in LWR primary circuits

The corrosion potential of stainless steels in LWRs primary circuits is determined by the nature and concentrations of oxidising (mainly oxygen and water radiolysis products such as hydrogen peroxide) and/or reducing species (mainly hydrogen), the water flow rate and the temperature. The state of the surface (oxidized, freshly machined, …) may also affect the corrosion potential to some extent.

3.1.1 PWR primary circuit

In PWR primary circuits, i.e. in an almost fully deaerated environment and in the presence of dissolved hydrogen, it has long been known that many materials including stainless steels act as a hydrogen redox electrode more than as a corrosion electrode (Figure 3-1) [Indig & Groot, 1969] and [Szklarska-Smialowska et al, 1991]. This is because the exchange current density of the H^+/H_2 reaction in high temperature water (several μA/cm² at ~300 °C according to [Cowan & Kaznoff, 1973]) is much higher (by more than an order of magnitude) than the oxidation current of stainless materials (Figure 3-2).

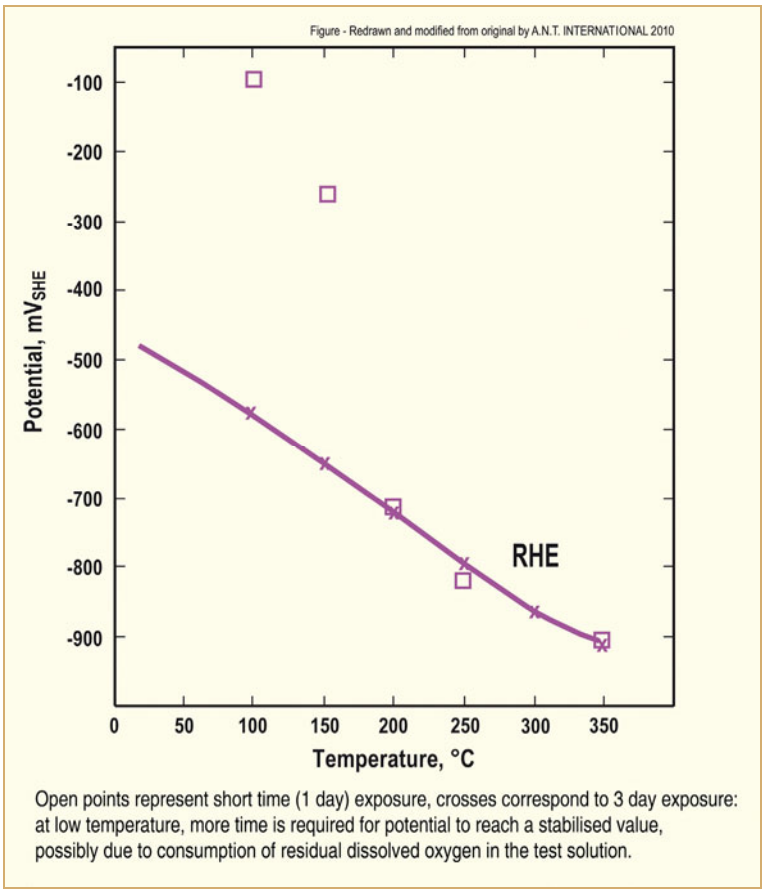

Figure 3-1: Corrosion potential of Type 304 stainless steel in lithiated, hydrogenated water compared to the Reversible Hydrogen Electrode (RHE) potential as a function of temperature [Szklarska-Smialowska et al, 1991].

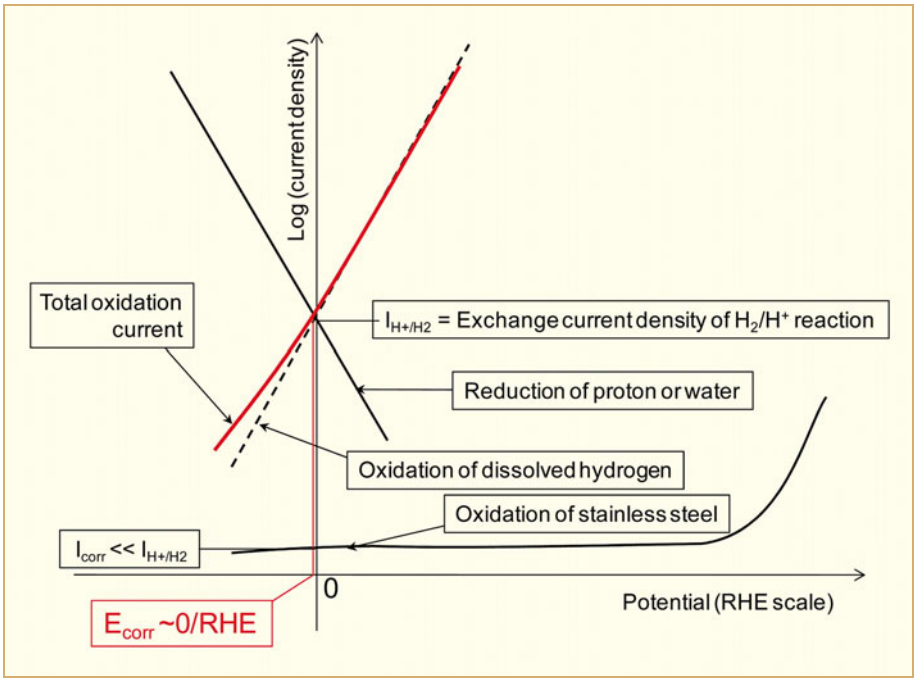

Figure 3-2: Evans diagram showing how the corrosion potential of stainless steel in PWR primary water is almost equal to the RHE potential because the exchange current density of the H^+/H_2 reaction is much higher than the oxidation current density of stainless steel.

This has the following consequences:

- Currents measured at the corrosion potential by linear polarisation techniques are representative of the H^+/H_2 reaction more than oxidation of stainless steel.
- Knowing the hydrogen content of the environment is sufficient to be able to calculate the corrosion potential versus the RHE with an accuracy of few mV without any direct measurement. If the pH at temperature is also known, the corrosion potential can also be calculated versus the Standard Hydrogen Electrode (SHE) at temperature.

3.1.2 BWR primary circuit

In BWR primary circuits with Normal Water Chemistry (NWC), water radiolysis leads to the presence of dissolved oxygen (typically 20 to 400 ppm) and hydrogen peroxide in the primary coolant (see Section 3.2 for a more detailed description of the effect of water radiolysis combined with stripping of non-condensable gases such as oxygen into the steam phase).

When increasing the oxygen content of the environment, the corrosion potential in high temperature water exhibits a pseudo threshold behaviour with the corrosion potential increasing rather abruptly from -700/-600 mV/SHE to - 200/+ 200 mV/SHE (Figure 3-3).

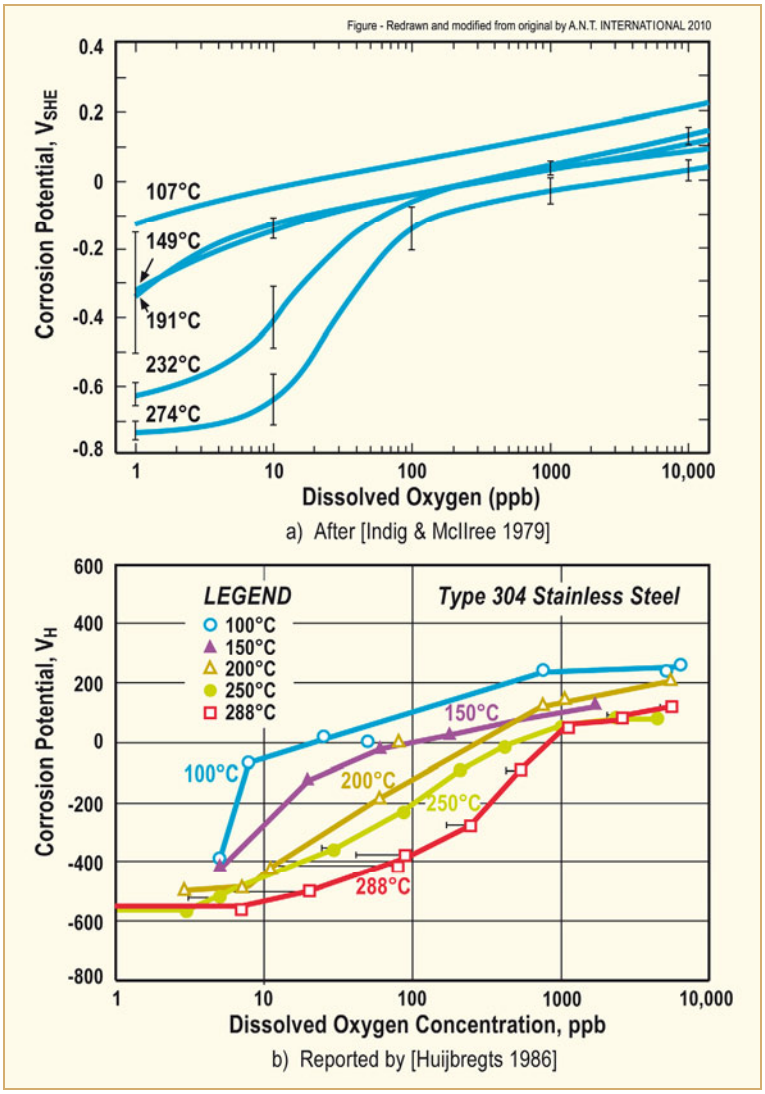

Figure 3-3: Corrosion potential versus dissolved O_2 and temperature for Type 304 stainless steels in pure water.

Another variable of major importance for the corrosion potential is the water flow rate past the metal surface. This is because the oxygen concentration at the surface and, therefore, the resultant cathodic reaction rate, is dominated by liquid diffusion control across the laminar flow boundary layer. The faster the flow velocity, the lower is the threshold oxygen concentration required for the corrosion potential to increase into the "high potential" range, as clearly shown in Figure 3-4 where the flow velocity is characterized in terms of Reynolds number. Consequently, "deaeration" of water has no intrinsic significance, its effect strongly depending on flow rate. Hence:

- At very high flow rates (Re ~10^7), 1 µg/kg of dissolved oxygen is sufficient for the environment to be "aerated", i.e. for the corrosion potential to be "high".
- At low flow rates (Re ~10^5), deaeration is effective in lowering the corrosion, potential for oxygen concentrations lower than ~10 µg/kg.
- At very low flow rates (Re < ~ 400), even an environment containing 100 µg/kg of dissolved oxygen behaves as if it is deaerated in terms of its effect on corrosion potential.

4 SCC of stainless steels under unirradiated and irradiated conditions in BWRs (Peter Ford)

4.1 Introduction

EAC is a materials degradation mode that encompasses SCC, strain induced corrosion cracking and corrosion fatigue, where these nomenclatures indicate the loading details; namely, constant stress (or strain), monotonically increasing strain and, finally, cyclic loading. As will be discussed later there is a spectrum of cracking susceptibility between these three submodes of EAC, all of which are encountered in LWR systems. They form an important subset of localized corrosion phenomena since the cracking is often hard to detect, and can have a severe impact on operational economics and, potentially, on plant safety.

The cracking morphology may be intergranular, granulated, interdendrittic or transgranular, and the morphology and degree of cracking susceptibility may change in any given alloy/environment system with relatively subtle changes in the combinations of material, stress and environment conditions. The interactions between these conditions are "conjoint"; that is, as illustrated schematically in Figure 4-1, all of the individual conditions must be met for a given degree of cracking susceptibility to be achieved.

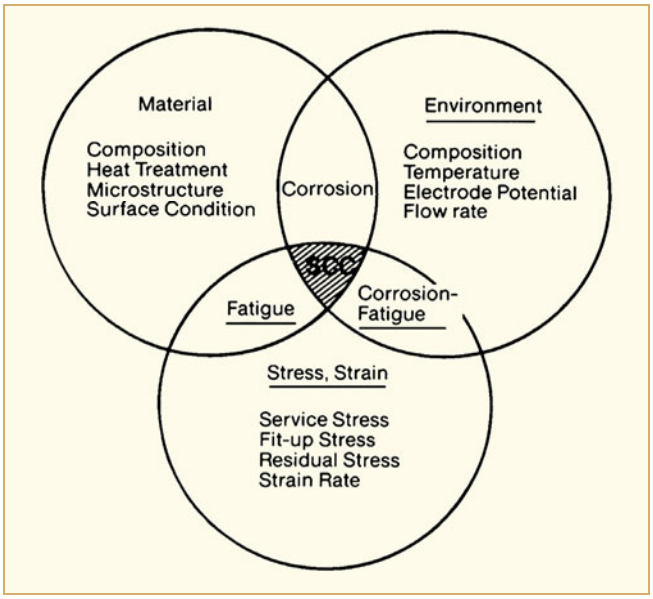

Figure 4-1: Conjoint material, stress and environment requirements for SCC [Speidel, 1984].

Such a Venn diagram was widely used in the 1970s and early 1980s to give a qualitative indication of the effect of the various system parameters on SCC of not only stainless steels, but also of nickel-base alloys and carbon and low-alloy steels. For example, the influence of each of the major material, environmental and stress factors could be represented by the diameter of each circle in Figure 4-1, and the resultant area of intersection of these three circles would then give some indication of the effect on cracking susceptibility (i.e. the shaded region in Figure 4-1). The limitation of this representation became apparent with the need for a more quantitative analysis of the benefits of various mitigation actions, and the realization that the actual cracking process was a good deal more complex than depicted in Figure 4-1. For example, system parameters such as cold work could affect two of the circles of influence (material and stress) independently, and irradiation could affect all three circles of influence.

Consequently, the qualitative understanding of cracking represented by Figure 4-1 was replaced by quantitative analyses of the effects of all the relevant system parameters, *and their interactions*, on cracking susceptibility. This Section concentrates on this development in the context of EAC of stainless steels in BWR environments.

In spite of the qualitative nature of Figure 4-1 it does indicate that there are two pieces of good news associated with this need for conjoint criteria for cracking to be sustained. The first is that it is unlikely that all the conditions will be met in all subcomponents in a broadly defined system, such as "*Welded Type 304 stainless steel recirculation piping in a Boiling Water Reactor (BWR)*". It is for this reason that, although the consequence of cracking may be significant, the frequency of occurrence of cracking in operating plant is not that great; less than 5% of all nominally similar welds in a given system[19] may crack in a specific time period, (Figure 4-2)[20]. The second piece of good news is that relatively small changes in the details of the "material", "stress" or "environmental" parameters can mitigate the problem and, in many cases, a "defence in depth" mitigation approach of positively modifying *two* of the system conditions has been adopted by many utilities (e.g. the use of Type 316NG stainless steel for replacement piping in BWRs, *plus* the implementation of HWC).

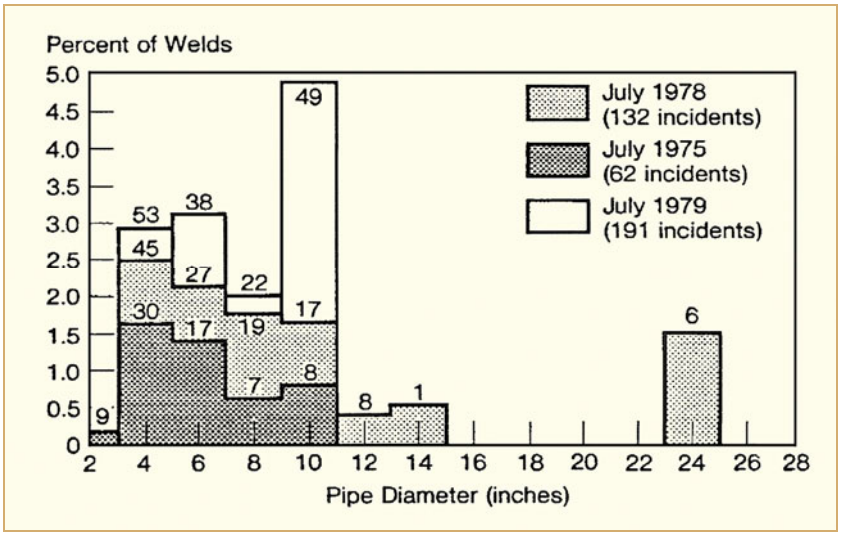

Figure 4-2: The frequency of IGSCC in BWR Type 304 stainless steel piping as a function of pipe size [Danko, 1991].

There are, however, two pieces of bad news. The first is that there is uncertainty in predicting the degree of susceptibility, since the actual system conditions may be ill-defined. The second is that, although the fraction of subcomponents exhibiting cracking may be small, for the reasons given above, the number and frequency of cracking incidents can increase with time because of the stochastic nature of some of the sub-modes in the cracking process. For example, pitting, which is a random, stochastic process, may have an impact on the timing on the subsequent cracking. In other words, the first observations of cracking are not necessarily "unique" and attributable to "unusual" operating or fabrication conditions and, more than likely, these "isolated incidents" are the beginning of a wave of similar incidents.

Before discussing the system-specific details, however, the chronology of cracking, which is common to most cracking incidents in structural materials in LWRs, is now addressed.

[19] IGSCC has been noted in the recirculation, core spray, residual heat removal, reactor water clean up, isolation condenser and control rod drive return lines.
[20] To put this into perspective the number of welds in these systems vary according to the specific design, from 300 in GE BWR-3 to 150 in GE BWR-6.

4.2 Chronology of processes common to stress corrosion systems

It is now recognized that the development of SCC in ductile alloys in LWR systems can follow a sequence of four distinct periods. Namely:

a) ***A precursor period*** during which specific metallurgical or environmental conditions may develop at the metal/solution interface that is conducive to subsequent crack initiation [Staehle, 2007a]. For example, the condition at the end of the precursor period may be pitting corrosion that causes breakdown of the normally protective surface oxide film leading to crack initiation (Figure 4-3 and Figure 4-4). Other precursor phenomena might be associated with the creation of localized environments within crevices or on heat transfer surfaces. These "precursor" periods may be very short if stresses are high, or if severe water impurity transients occur during initial reactor operations. An example would be the cracking of weld-sensitized Type 304 stainless steel BWR piping whose surface had been ground following welding in order to facilitate ultrasonic inspection. On the other hand, the precursor events may take years if they are associated with a change in metallurgical microstructure involving thermal aging, irradiation embrittlement, grain boundary diffusion or oxidation, or the creation of the necessary stress due to corrosion product formation and expansion. While the mechanism of degradation during the precursor period may be closely related to the processes that control cracking during subsequent stages, they can also be entirely different depending on the details of the breakdown of the surface film. If this latter situation is the case then analyses of times to failure can be complicated, especially if the system conditions are changed during the component lifetime.

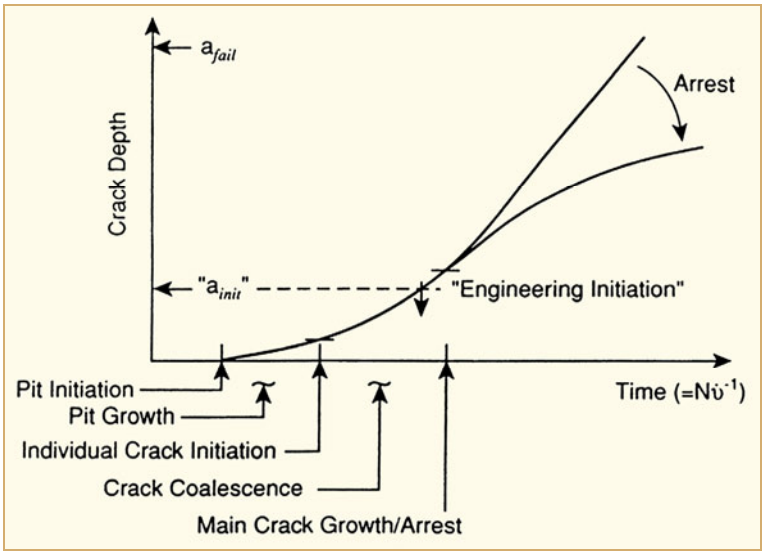

Figure 4-3: Sequence of crack initiation, coalescence and growth during sub-critical cracking in aqueous environments. Note the arbitrary definition of "Engineering Initiation" which generally coincides with the NDE resolution limit.

b) **The initiation of cracks** when the local environment, microstructure, stress and crack geometry conditions have reached a critical state. An example is shown in Figure 4-4, where a transgranular corrosion fatigue crack in a mild steel, stressed in partially oxygenated 288 °C water (symptomatic of BWR coolant), has initiated at a pit that was formed at lower temperatures (symptomatic of reactor shut down or lay-up conditions). The size and spacing of the crack initiation sites will depend on the distribution of surface breaking MnS precipitates, machining marks, cold work and stress raising sites, (such as sharp radius stress concentrations at bolt heads or the presence of re-entrant angles at welds between misaligned pipes).

5 IGSCC/IASCC of cold worked/irradiated and high strength stainless steels in de-oxygenated PWR-type coolants (Peter Scott)

Type 304L and 316L stainless steels (Table 2-2) are the main materials used for primary coolant piping and other components exposed to primary coolant in PWRs (and BWRs). CASS with similar compositions (designated CF-3, CF-3M and CF-8) have also been widely used for large diameter primary piping, elbows and nozzles in PWR primary circuits. Operating experience with respect to environmental degradation of all these low strength materials in PWRs since the mid-1960s has generally been excellent. The only major concerns that have been raised are with thermal ageing and embrittlement of some of the cast austenitic grades, see Chapter 1, and with the effects of irradiation on core support structures, as described here in Section 5.2.

SCC of the low strength austenitic stainless steels has been comparatively rare in PWR primary service and when it has occurred in the absence of irradiation, in most if not all cases, the cause has been internal or external surface contamination by chlorides or out-of-specification chemistry in dead-legs or other occluded volumes. These cases of SCC involving external surface contamination or localised departures from the PWR primary water specification are reviewed in detail in Section 6.4.2. In a few cases, it has been claimed that SCC may have occurred in normal quality PWR primary water but these cases concern austenitic stainless steels that have been significantly cold worked, as reviewed here in Section 5.1.

Where higher strength is necessary (for bolts, springs, valve stems etc.), PH A 286 austenitic stainless steel, or martensitic stainless steels, or PH martensitic stainless steels have been used. Environmentally induced cracking of these materials has usually been attributed to excessive hardness and strength on entering service or, in the case of PH martensitic stainless steels, to thermal ageing and hardening in service. Operating experience and associated laboratory studies of these materials are reviewed here in Section 5.3.

5.1 Austenitic stainless steels – effects of cold work

5.1.1 Operating experience

Since the widespread problems that occurred with thermally sensitized weld HAZs of austenitic stainless steels in BWRs in the 1970's (see Section 3.1), the normal fabrication practice has been to use low carbon grades of Types 304 and 316 stainless steels in both PWRs and BWRs. An alternative adopted in some countries has been to use niobium or titanium stabilized grades such as, respectively, Type 347 or Type 321, where the carbon is trapped as stable niobium or titanium carbides, which are very resistant to sensitization. Nevertheless, there is little doubt that in many older PWRs sensitized Type 304 and 316 stainless steels exist in considerable quantities but practical experience shows that de-oxygenated, hydrogenated PWR primary water does not cause SCC, in contrast to BWR experience with oxygenated NWC coolant. The reason is clearly related to the presence of dissolved hydrogen in PWR primary circuits, which ensures that corrosion potentials are close to the hydrogen/water redox potential and well below the desired protection potential identified for thermally sensitized stainless steels in BWRs (Section 3.1). The exceptions in PWRs primarily concern certain dead legs where air bubbles may be trapped during refuelling, as discussed in detail in the following Chapter 6 Section 6.4.

More recently, however, concerns have emerged about the possible stress corrosion susceptibility of cold worked stainless steels even at low corrosion potentials in flowing, normal quality PWR primary water [Ilevbare et al, 2007]. One of the most recent incidents to fuel this interest in the possible susceptibility of austenitic stainless steels to SCC in PWR primary water was a leak of primary water that was clearly due to IGSCC of a Type 316 pressurizer heater tube at the Braidwood Unit 1 PWR [Chynoweth & Hyres, 2007]. Destructive examination showed that through wall circumferential cracking had developed from the ID through the HAZ of a socket weld, which appeared to be sensitized. Very recently, a single shallow circumferential intergranular crack was discovered in the HAZ of a Type 316 safe end of a dissimilar metal weld between a steam generator and the primary water inlet piping at Mihama 2 (during an intervention whose primary purpose was to apply a remedial surface treatment to the nickel-based Alloy 132 weld) [JANTI, 2008]. On the other hand, no cracking occurred on the primary water coolant side of the Type 308 stainless steel weld overlay cladding of a PWR pressure vessel despite dynamic straining caused by bulging of the cladding following loss of the low alloy steel support due to boric acid corrosion [Xu et al, 2005].

An analysis of PWR operating experience of SCC in austenitic stainless steels has shown that 85% of 146 recorded cracking events in austentitic stainless steel were due to localised perturbations to primary water chemistry in occluded volumes [Ilevbare et al, 2007]. However, the remaining 15% appeared to show that intergranular or mixed intergranular/transgranular stress corrosion cracking (IGSCC/TGSCC) had occurred without any obvious departure from PWR primary water specifications. The 15% of events concerned mainly pressurizer heater sleeves or cladding and heat exchanger tubing in the CVCS. There also appeared to be a clear association between the incidence of cracking and hardness >300 HV but sensitization was clearly not a risk factor.

Despite a growing body of experimental data reviewed in Section 5.1.2 that clearly shows that austenitic stainless steels can crack in normal quality PWR primary water if they are sufficiently cold worked, in the opinion of this author, the above analysis of operating experience omits some key information that points to another likely culprit.

Firstly, deliberately strain hardened stainless steels, mainly Type 316 and to a lesser extent niobium stabilized Type 347, have been used for many decades in PWRs for bolting and other purposes where moderate strength is required, and without apparent problems except when highly irradiated (see Section 5.2.1). However, a limit is imposed on the maximum yield strength of such deliberately strain hardened components of 90 ksi (or 625 MPa) [USNRC, 2007a]. In practical terms for unstabilized austenitic steels with medium carbon content, this corresponds to an upper limit on cold work of ~20% or a hardness of ~300 HV. As noted in Section 5.3, stress corrosion of other hardenable, high strength, stainless steels only becomes apparent in service at hardness values greater than ~350 HV.

Secondly, the particular austenitic stainless steel components that have been identified with SCC have other possibilities for coming into contact with out-of-specification primary water chemistry. For example, in heater/support plate crevices in pressurizers the occluded aqueous environment can become strongly alkaline at very low boric acid concentrations at the end of a fuel cycle and particularly during cycle stretch-out. Both pressurizers and CVCS heat exchanges are also vulnerable to air-saturated make-up water ingress due to a growing practice not to de-aerate the make-up water tanks of PWRs as the original vendors intended. This modification to operating practice now affects about half the operating PWR fleet and it is this make-up water that flows through the CVCS heat exchangers to a spray nozzle in the pressurizer (as well as to the main circulating pump shaft seals and the CVCS nozzle in the primary circuit cold leg). Given the history of SCC of cold worked stainless steels in BWRs (Section 3.1), this seems a much more likely explanation to this author of the incidents cited above. Moreover, laboratory testing shows that if oxygen is allowed to contaminate PWR primary water so that the corrosion potential rises to values normally associated with BWRs, then IGSCC will start to propagate rapidly in sensitized austenitic stainless steels after only ~10 hours exposure to the oxygen contaminated primary water [Andresen & Morra, 2001] and [Andresen & Morra, 2007c].

5.1.2 Laboratory tests

Interest in laboratory studies of SCC of cold worked austenitic stainless steels in PWR primary water has arisen mainly since 2000, firstly as a potential analogue of irradiated stainless steels without the testing problems associated with highly neutron activated materials, and secondly in direct support for the in-service incidents described in the previous section. In addition, by analogy with BWR experience of IGSCC adjacent to the fusion lines of austenitic stainless steel welds due to strain hardening in non-sensitized HAZs (see Section 3.1), there are concerns that longer term problems could similarly arise in PWRs. Two main testing approaches have been used: the SSRT, also often called the CERT, and crack propagation rate measurements on fatigue pre-cracked fracture mechanics specimens. It has to be said that the SSRT does not seem to be that well adapted to this problem because plastic strain introduced during testing will obviously change the amount of cold work in the material. Thus, only interrupted SSRTs, where the additional cold work introduced during the SSRT is small relative to the starting cold work condition, are likely to be very informative with regard to the dependence of the observables on prior cold work.

Despite the reservations expressed in the preceding paragraph about the use of the SSRT in this context, several studies have shown that prior cold work of Type 304L or 316L stainless steels, does lead to susceptibility to mixed IGSCC plus TGSCC in simulated PWR primary water [Kaneshima et al, 2002], [Arioka, 2002] and [Arioka et al, 2003]. Susceptibility to SCC increases with increasing prior deformation ratio in tests usually conducted at strain rates around 10^{-7} s^{-1} on tensile specimens with prior cold work in the range 20 to 60%. The SSRT straining is usually in the same direction as the prior cold work and test temperatures are typically 340 to 360 °C. A variation on this test technique, which seems particularly favourable for promoting IGSCC, is to use the so-called 'hump' specimen where a V-shape deformation is introduced into the gauge length of the specimen prior to the SSRT. In this case, the cold work condition in the hump is particularly high and complex. The effects of environmental chemistry of PWR water have been studied by SSRT using hump tensile specimens of Type 316 stainless steel [Arioka, 2002] and [Arioka et al, 2003]. A small but monotonic increase in SCC susceptibility was observed as a function of hydrogen concentration in the normal range for PWR primary water at 320 °C but increasing boric acid was observed (surprisingly) to strongly suppress SCC susceptibility. An activation energy of ~90 kJ/mole was also measured in this work and is about half that associated with PWSCC of Alloy 600, for example, while deliberately heat treating the material to form grain boundary carbides (i.e. sensitization) was observed to have a favourable influence on SCC susceptibility. The latter result was deduced to indicate that grain boundary sliding was involved in the mechanism and was seemingly supported by creep tests in air at 440 to 560 °C.

Some considerable effort using the SSRT, constant strain and constant load testing has been put into studying the effect of different methods of introducing cold work into austenitic stainless steels [Raquet et al, 2005], [Couvant et al, 2005] and [Couvant et al, 2007a]. Cold working by shot peening, rolling, fatigue, pre-shearing, milling and tensile deformation have been studied and work has also been undertaken to elucidate the influence of the so-called 'strain path'. Two pre-conditions are necessary for SCC to initiate and propagate in Type 304L or 316L stainless steels in simulated PWR primary water (at 320 or 360 °C); a hardness > 300 to 310 HV (i.e. an equivalent stress of ~700 MPa) and dynamic straining. However, no significant creep occurs at 360 °C (i.e. $<3x10^{-12}$ s^{-1} for true stresses between 200 and 400MPa). It is interesting to note that the hardness threshold observed by SSRT (~310 HV) is significantly lower than that deduced from in-service behaviour of high strength stainless steels (~350 HV) discussed here in Section 5.3, or indeed that observed in laboratory testing in oxygenated BWR water (~340 HV), Figure 5-1 [Tsubota et al, 1992]. Noting that severely cold worked austenitic stainless steels up to hardness values of 450 HV have not cracked in the laboratory at constant load in simulated PWR primary water [Raquet et al, 2005], underscores even more the likelihood that in-service incidents in PWR primary circuits could be linked to the ingress of aerated water, as discussed earlier in Section 5.1.1. However, at hardness values >350 HV, hydrogen embrittlement cannot be excluded in the absence of oxygen, particularly at intermediate temperatures of ~150 °C.

6 Corrosion of stainless steels in contaminated LWR environments (Pierre Combrade)

6.1 Background

Stainless steels are present not only in the main circuits of LWR, i.e. in contact with the PWR or BWR primary coolants, but also in many auxiliary circuits where the probability of contamination is often much higher.

General corrosion of stainless steels is not a concern for the structural integrity of the circuits in the near neutral environments that prevail in LWRs. However, it is of major importance for the radioactivity of the primary PWR and BWR circuits since it contributes to the source term of metallic cations that can be activated in the reactor core. This problem has been described by Riess (See annual report LCC1) and Wood (see annual report LCC4).

Due to the nature of their Cr-rich compact passive films, stainless steels are usually not susceptible to flow-assisted corrosion unless the passive film is mechanically damaged, for example by impingement, cavitation or erosion by solid particles.

However, in presence of impurities in the operating environment and/or external surface contaminants, stainless steels may, like all passive materials, be susceptible to passivity breakdown that can lead to different forms of localised corrosion, mostly intergranular corrosion, pitting and crevice corrosion and to Microbiologically-Induced Corrosion (MIC). In addition, the presence of impurities may also cause SCC[32].

Among the impurities that may be deleterious for stainless steels, the most aggressive and the most widespread is quite clearly **the couple chloride ions/dissolved oxygen** that is well known to cause pitting and crevice corrosion and, in the case of austenitic stainless steels, SCC. However, sulphur ions can also be very damaging and they are involved in a significant number of corrosion incidents of stainless steels in LWRs.

6.2 Intergranular corrosion of sensitized stainless steels

Sensitization of austenitic stainless steels results from heating in a range of temperature, typically 500 to 800 °C, which causes intergranular precipitation of chromium carbides and chromium depletion of the base metal adjacent to the grain boundaries. This phenomenon, which is of major importance in the primary circuit of BWRs, has been described by Ford in LCC2, in the STR "Environmentally Assisted Degradation of Structural Materials in Water Cooled Reactors" and in Chapters 2 and 4 of this report.

As a consequence, resistance to corrosion of the Cr-depleted zones, particularly in acidic environments, is impaired and preferential dissolution may occur. This can cause intergranular failure of the material with only a limited loss of metal.

In LWRs, in addition to IGSCC in BWRs, sensitisation of stainless steels may lead to material degradation, mainly in the presence of reactive sulphur species such as polythionates that can be formed for example from resin decomposition in high temperature water and may cause very severe intergranular damage to sensitised stainless steels (and nickel base alloys) either as uniform integranular corrosion or as SCC at temperatures close to ambient.

[32] SCC is often considered as a form of localised corrosion. However, we prefer to consider SCC as a separate form of corrosion because, in many cases, and in particular in chloride environments, it very likely involves brittle micro-ruptures of the base metal (see for example the Corrosion Enhanced Plasticity Model developed for stainless steels in chloride environments).

Today, the use of low carbon austenitic stainless steels and/or the addition of Ti or Nb to "stabilise" stainless steels by immobilizing free carbon (and nitrogen) in stable Ti(C,N) or Nb(C,N) precipitates avoids most intergranular corrosion and cracking problems related to contaminated environments.

A similar problem related to intergranular chromium depletion may affect ferritic stainless steels. Since carbon solubility is lower and diffusion coefficients are higher in ferrite than in austenite, sensitization occurs in a lower temperature range and for shorter times, so that it is very difficult or even impossible to avoid during cooling down after solution annealing treatment. The practical solution to avoid sensitization is to heat treat ferritic stainless steels at temperatures of ~800-850 °C to avoid significant carbide dissolution.

6.3 Localised corrosion in chloride environments: Pitting and crevice corrosion

Localised corrosion of stainless steels occurs when a galvanic couple can be stabilised between an **occluded cell** within which no oxidiser other than water is present to take part in a cathodic reaction, and an external surface where the reduction of an oxidising species can balance excess anodic current in the occluded cell. One consequence of the potential gradient between the occluded cell surfaces and the external free surfaces is mass transport by electromigration of anions from the bulk solution towards the occluded cell and of cations towards the free surfaces outside the occluded cell, as shown in Figure 6-1 for the case of an aerated chloride solution. Hydrolysis of dissolved metallic cations within the occluded cell, combined with the transport of anions towards the occluded cell may result in a local drop of pH[33] and a very high concentration of chloride and hydrolysed metallic cations.

Accordingly, localised corrosion may occur only when two conditions are met simultaneously:

i) An oxidising species other than water is dissolved in the bulk environment and is depleted within the occluded cell.

ii) A strong acid forming anionic species is present in the bulk solution that can allow a low pH to develop in the occluded cell, e.g. chloride or sulphate ions.

[33] Also an increase of pH on the free surfaces close to the occluded cell. Due to the relatively large surface area outside the occluded cell, this pH increase on the external surface usually has no significant effect. On Figure 6-2, it can be seen that it may cause precipitation of (hydrated) oxides that would otherwise be soluble at the pH of the bulk environment.

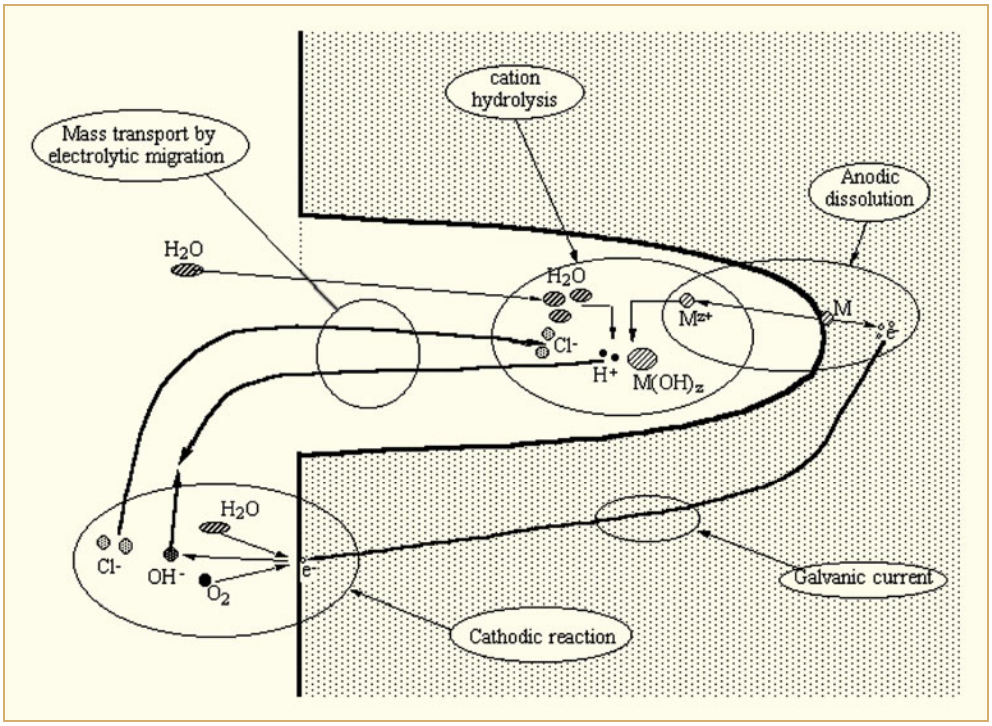

Figure 6-1: Sketch of the main reactions and transport processes in the propagation stage of localised corrosion of stainless steels in chloride environments [Combrade, 2001]. Note that cation hydrolysis is written in an oversimplified form since it actually produces complex metallic hydroxichlorides.

This mechanism can lead to localized corrosion of stainless steels only if the anions that concentrate in the occluded cell are deleterious to passivity, i.e. are able of causing breakdown of existing passive layers (which is the case of chloride ions) or of inhibiting the formation of passive layers on active surfaces (which is the case of active sulphur species such as sulphide, thiosulphate, thiocyantes, tetrathionate, … ions). Sulphate ions for example can cause a pH drop in occluded cells but are not deleterious to passive layers and, thus, very rarely cause localized corrosion by themselves.

One important consequence is that in PWR primary water no localised corrosion due to electrochemical cells can occur in deaerated nor, indeed, in aerated conditions. This is because:

i) In deaerated conditions, the cathodic reaction is the reduction of water or of protons and occurs both inside and outside the occluded cell.

ii) In aerated conditions, boric acid is a too weak an acid to allow very low pHs to develop inside occluded cells where it may even have some buffering effect against modest Cl^- intrusion.

In BWR water, which contains dissolved oxygen and hydrogen peroxide but normally no significant concentrations of anionic species, localised corrosion is also impossible due to the very low level of ionic species that could cause a drop of pH in occluded cells. Indeed, to our knowledge, no case of localised corrosion has been reported in BWR primary circuits[34].

[34] However, the concentration of impurities in cracks may be large enough to play a major role in IGSCC phenomena that does not require a local environment that is aggressive enough to cause passivity breakdown in the absence of strain.

7 Corrosion fatigue (Peter Ford and Peter Scott)

In the discussion so far of EAC, it has been assumed that the structures are predominantly under constant stress or strain loading conditions. In fact, many LWR structures are exposed to cyclic loading because of changes in mechanical and thermal conditions. These cyclic loading conditions span a wide range of strain amplitudes, loading frequencies, mean stress values, and this variety has led to a categorization of fatigue phenomena, such as "High Cycle Fatigue", "Low Cycle Fatigue", "Thermal Fatigue" and "Environmental (or Corrosion) Fatigue". Such cyclic loading phenomena have presented an on-going problem to LWRs, as reviewed in 1997, [Garud et al, 1997].

The category, "High-cycle Fatigue", refers to a high number of cycles at a relatively low stress amplitude (typically below the material's yield strength, but above the fatigue endurance limit[39] of the material), with the driving force for the cyclic loading coming from, for example, high frequency flow-induced vibrations and/or instabilities in thermal mixing of the hot and cold parts of the coolant. These may be experienced at feedwater nozzles, for example. On the other hand, "Low-cycle Fatigue" refers to the higher stress/strain amplitude regime, where the local yield stress may be exceeded leading to correspondingly shorter fatigue lives. Such a regime is often associated with lower frequency operational transients such as plant start-up/shut-down or hot stand-by. "Thermal Fatigue" is due to cyclic stresses/strains associated with changing temperatures in a component or piping attached to the component and may occur under both Low and High-cycle fatigue conditions (involving, respectively, a relatively low number of cycles at a higher stress or a high number of cycles at low stress amplitude such as local leakage effects or cyclic stratification).

"Environmentally–Assisted (or Corrosion) Fatigue" encompasses the effect of the aqueous environment on fatigue, and is usually associated with cyclic loading in the lower frequency range. The process can be complex since the environment can affect all of the events in the cracking chronology illustrated in Figure 4-3. Indeed, corrosion fatigue cracks in carbon steels in high temperature water can initiate at pits, exactly as do stress corrosion cracks (Figure 4-4), and these then propagate, slow down, coalesce and then accelerate (Figure 7-1).

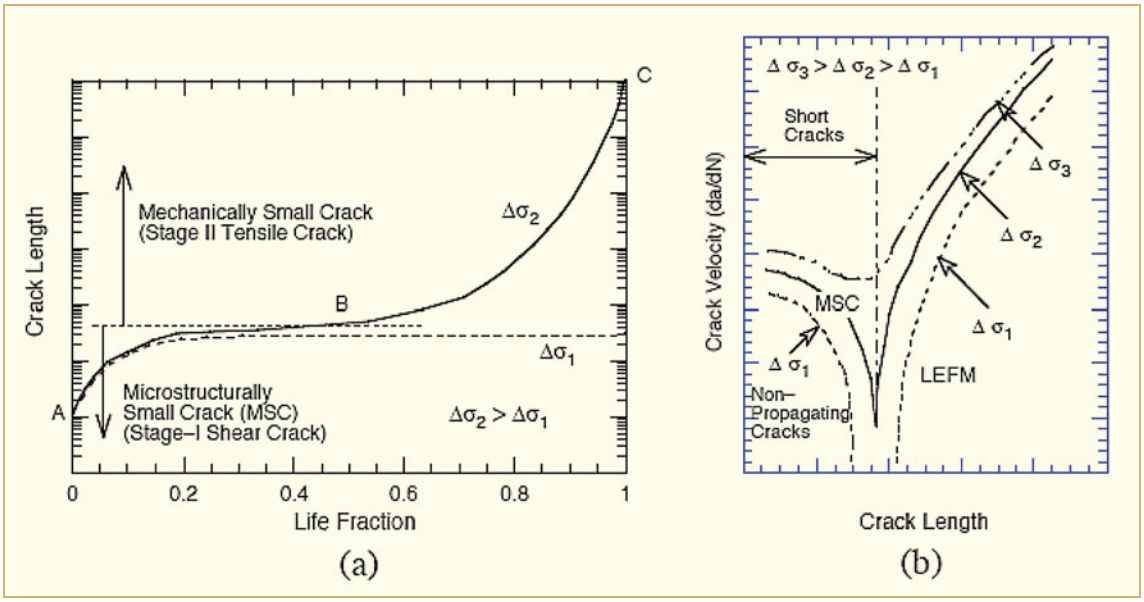

Figure 7-1: Schematic illustration of (a) growth of short cracks in smooth specimens as a function of fatigue life fraction and (b) crack velocity as a function of crack length [Ford, 2006].

[39] Usually defined as the strain or pseudo-elastic stress amplitude at 10^7 cycles

As mentioned previously in Chapter 4, corrosion fatigue can be viewed as an extension of SCC and strain-induced corrosion cracking in the overall spectrum of EAC modes. In this case, however, it is recognized that the environmental component of crack advance is superimposed on a component of crack advance due to "mechanical fatigue" that would occur in an inert environment. This spectrum of cracking responses between SCC, strain-induced corrosion cracking and corrosion fatigue is illustrated in Figure 4-18 where it is seen that there is a monotonic increase in the crack propagation rate with increasing crack tip stain rate associated with different loading modes. It is also apparent (Figure 4-19) that the change in the crack propagation rate in changing from one environment to another becomes less as the crack tip strain rate increases.

The specific effects of environment on fatigue behaviour of stainless steels in LWR environments are discussed below in terms of "crack initiation" and crack propagation. Although this division is somewhat arbitrary, it is justifiable given the impact on initial design decisions (where the avoidance of crack initiation is being addressed) and decisions regarding continued operation if a crack is detected.

7.1 Crack initiation

As discussed in Section 4.3, an analysis of fatigue resistance forms part of the design basis for LWRs, which in the USA is in accordance with Appendix 1 of Section III of ASME Pressure Vessel Code [ASME, 1969]. As such, it is therefore subject to a regulatory Time Limited Aging Analysis (TLAA) when the design basis is changed due to, for example, power uprates or life extension. Very similar requirements exist in other countries.

Fatigue life is calculated from strain-amplitude versus crack initiation time (or cycles) relationships whose bases are fatigue data measured on smooth cylindrical specimens, cyclically loaded under strain control. "Initiation" in this case is defined as a drop in maximum load by 25%, which physically corresponds to a crack of approximately 1-3 mm depth, with the absolute value depending on the geometry of the laboratory specimen. Examples of these relationships for tests in air at various temperatures are shown in Figure 7-2a and Figure 7-2b for Type 304 and 316 stainless steels [Chopra & Shack, 2006] where the data are compared with best fit correlations from Argonne National Laboratory (ANL) and from ASME. Note that the ASME relationship is based on data obtained at 25 °C. It is concluded that temperature, at least up to 456 °C, does not have a major impact on the mean data set determined in air. There is however, a difference in the ANL and ASME relationships for strain amplitudes < 0.3%. This is attributed to differences in the tensile strengths of the steels used in the relatively restricted data base used to define the "ASME Code mean curve" and the expanded data base from various laboratories in Japan, France, and the USA that was used to define the "Best Fit Air ANL Model" [Chopra & Shack, 2006].

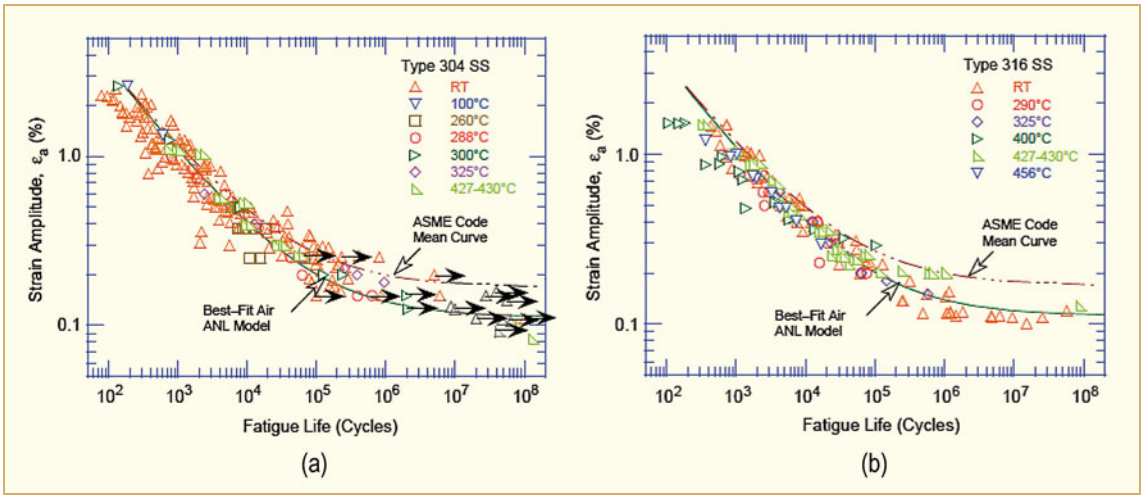

Figure 7-2: Fatigue strain amplitude versus cycles for (a)Type 304 and (b) Type316 stainless steel at various temperatures in air [Chopra & Shack, 2006].

The strain amplitude versus cycles to crack initiation in air relation adopted by ANL and the USNRC, and against which environmental effects will be compared, is given by:

Eq. 7-1: $$\ln(N) = A - 1.92 \ln(\varepsilon_a - 0.112)$$

The value of the parameter A is distributed as indicated in Figure 7-3, with a median value of 6.891. This distribution accounts for various heats of stainless steel and temperatures up to 400 °C.

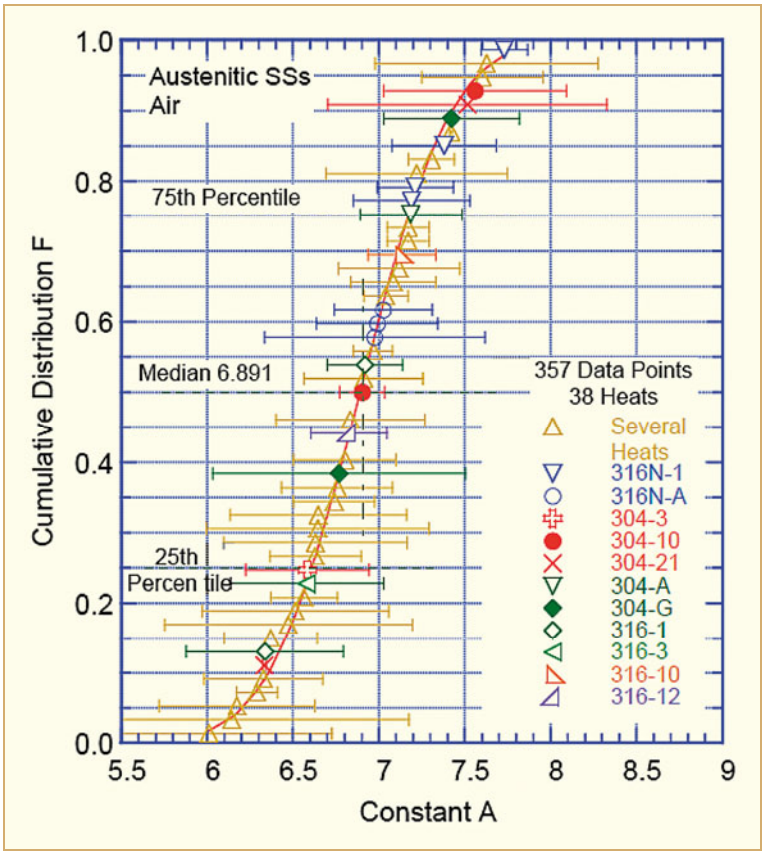

Figure 7-3: Cumulative distribution of the parameter A in Eq. 7-1 taking into account variations in temperature and stainless steel heats [Chopra & Shack, 2006].

The original ASME *design* curve for fatigue crack initiation was based primarily on a fatigue data curve obtained in air at 25 °C and offset by a specific amount to account for various factors such as the unknown (in 1969) effects of temperature, surface roughness, environment, etc. These corrections were regarded not as safety factors but as "adjustment factors" [Cooper, 1992] that were applied to small laboratory specimen data in order to make reasonable estimates of the fatigue lives of large industrial components.

Based on engineering judgment, the "design curve" was displaced from the room temperature air curve by a factor of 2 (on stress/strain amplitude) or 20 (on fatigue life), whichever was the more conservative [ASME, 1969]. The origin of the factor of "20" arose out of presumed effects of data scatter, specimen size, surface finish, etc.:

Scatter in data (minimum to mean)	factor 2.0
Size effect	factor 2.5
Surface finish, atmosphere, etc.	factor 4.0

8 References

Ahlberg E. and Rebensdorff B., In Proc. BNES Conf. Water Chem. Nucl. Reactor Syst. 6, Bournemouth, UK, 12-15 Oct. 1992, Vol.2, 278-5/8, 1992.

Akashi M. and Nakayama G., "*Stress Corrosion Crack Initiation Process Model for BWR Plant Materials*" in"*Plant Aging and Life Prediction of Corrodible Structures*", Eds T.Shibata and T. Shoji, pp. 99-106, Sapporo, 1995.

Alexander J. E., "*Alternate Piping Alloy Qualification",* EPRI Report WS-79-174 Vol.1 May 1980.

Alexander J. E., "*Alternative Alloys for BWR Pipe Applications*", EPRI NP-2671-LD, Electric Power Research Institute, October 1982.

Amman F., "*Remedial Measures against MIC*", Presentation to European Workshop on Microbially Influenced Corrosion, Erlangen Germany, 2006.

Ando M.and Nakata, "*Crack Growth Rate Behaviour of Low Carbon Stainless steels of Hardened Heat Affected Zone in PLR Piping Weld Joints*", Proc. 13th Int. Symp. on Environmental Degradation of Materials in Nuclear Power Systems – Water Reactors", Whistler BC, August, 2007.

Andresen P. L. "*The Effects of Surface Preparation, Stress and Deaeration on the Stress Corrosion Cracking of Type 304 Stainless Steel in Simulated BWR Start-Up Cycles*", Proceedings of Seminar on Countermeasures for Pipe Cracking in BWRs, Vol. 3, January 22-24, 1980. EPRI Reports WS 79-174, May 1980.

Andresen P. L. and Duquette D. J., "*The Effect of Chloride Ion Concentration and Applied Potential on the SCC Behavior of Type 304 Stainless Steel in Deaerated High Temperature Water*", Corrosion, 36, 2, 85, 1980.

Andresen P. L., "*The Effects of Aqueous Impurities on Intergranular Stress Corrosion Cracking of Sensitized 304 Stainless Steel*" EPRI Report NP-3384, November 1983.

Andresen P. L., "*Effect of Material and Environmental Variables on Stress Corrosion Crack Initiation in Slow Strain Rate Tests on Type 304 Stainless Steel*", Symp. On Environmental Sensitive Fracture; Evaluation and Comparision of Test Methods, April 1982. Published in ASTM STP821 pp. 271-287, 1984a.

Andresen P. L., "*Laboratory Results on Effects of Oxygen Control During a BWR Start up on the IGSCC of 304 Stainless Steel*", Proceedings of Second Seminar on Countermeasures for Pipe Cracking in BWRs, November 15-18, 1983. EPRI Report NP-3684-SR Sept. 1984 Vol 2, p. 12-1 1984b.

Andresen P. L, "*Modeling of Water and Material Chemistry Effects on Crack Tip Chemistry and Resulting Crack Growth Kinetics*", Proc. 3rd Int. Conf. Environmental Degradation of Materials in Nuclear Power Systems - Water Reactors, Traverse City, AIME, pp. 301-314, 1987.

Andresen P. L., Ford F. P., Murphy S. M., Perks J. M., "*State of knowledge of radiation effects on environmental cracking in light water reactor core materials*", pp. 1-83 to 1-121, Proceedings of the 4th Conference on Environmental Degradation of Materials in Nuclear Power Systems – Water Reactors, Jeckyll Island, GA, August 1989, (NACE, Houston, 1990a).

Andresen P. L., Vasatis I. P. and Ford F. P., "*Behavior of Short Cracks in Stainless Steel at 288 ℃*", Paper 495, NACE Conference, Las Vegas, April 1990b.

Andresen P. L., "*Effects of Specific Anionic Impurities on Environmental Cracking of Austenitic Materials in 288 °C Water*" in Proceedings of Fifth International Symposium on Environmental Degradation in Nuclear Power Systems – Water Reactors. Monterey August 25-29,1991 Eds.D. Cubicciotti, E.Simonen. Published, by American Nuclear Society. ISBN 0-89448-173-8, pp. 209-218, 1991.

Andresen P. L. "*Effects of Zinc Additions on the Crack Growth Rate of Sensitized Stainless Steel and Alloys 600 and 182 in 288 Water*", Paper 72, Water Chemistry of Nuclear Reactor Systems 6, BNES, London, 1992a.

Andresen P. L., "*Effect of Temperature on Crack Growth Rate in Sensitized Type 304 Stainless Steel and Alloy 600*", Paper 89 NACE Corrosion -92, Nashville, April 1992b.

Andresen P. L., "*Effect of specific anionic impurities on environmental cracking of austenitic materials in 288 °C water*", 5th International Symposium on Environmental Degradation of Materials in Nuclear Power Systems — Water Reactors, Monterey, August 1991, ANS, La Grange Park, IL, 209, 1992c.

Andresen P. L., "*Stress Corrosion Cracking – Material Performance and Evaluation*", Ed. R. H. Jones ASM, p. 181, 1992d.

Andresen P. L. "*Specific Anion and Corrosion Potential Effects on Environmentally Assisted Cracking in 288 °CWater*", GE-CRD Report 93CRD215, December1993a.

Andresen P. L. "*Effects of Dissolved Silica on the Crack Growth Rate of Sensitized Stainless Steel*", GE-CRD Report 93CRD212, December 1993b.

Andresen P. L., "*The Effects of Nitrate on the Stress Corrosion Cracking of Sensitized Stainless Steel at 288C*", GECRD Report 93CRD213, December 1993c.

Andresen P. L., "*Effects of Nitrate on the Stress Corrosion Cracking of Sensitized Stainless Steel in High Temperature Water*", in Proceedings of Seventh International Symposium on Environmental Degradation in Nuclear Power Systems – Water Reactors, Eds.R. Gold, A. McIlree. Published by National Association of Corrosion Engineers. ISBN 0-877914-95-9, pp. 609-619, Breckenridge, August 7-10, 1995a.

Andresen P. L., "*Application of Noble Metal Technology for Mitigation of Stress Corrosion Cracking in BWRs*", Proc. 7th Int. Symp. on Environmental Degradation of Materials in Nuclear Power System-Water Reactors, pp. 563, NACE, Houston, TX, 1995b.

Andresen P. L. and Angeliu T. M. "*Effects of Zinc Additions on the Stress Corrosion Crack Growth Rate of Sensitized Stainless Steel, Alloy 600 and Alloy 182 Weld Metal in 288 °C Water*", Paper 409, Corrosion-95 NACE, Orlando, March 1995.

Andresen P. L. and Ford F. P. "*Modeling and Prediction of Irradiation Assisted Cracking*" in Proceedings of Seventh International Symposium on Environmental Degradation in Nuclear Power Systems – Water Reactors. Breckenridge, Eds.R. Gold, A. McIlree. Published by National Association of Corrosion Engineers. ISBN 0-877914-95-9, pp. 893-908, August 7-10, 1995.

Andresen P. L. and Young L. M. ,"*Crack Tip Microsampling and Growth Rate Measurements in Low Alloy Steel in High Temperature Water*", Corrosion Vol 51, no. 3, pp. 223-233, March 1995.

Andresen P. L, Ford F. P, Higgins J. P, Suzuki I., Koyama M., Akiyama M., Okubo Y., MishimaY, Hattori S., Anzai H., Chujo H. and Kanazawa Y., "*Life Prediction Of Boiling Water Reactor Internals*", Proc., ICONE-4 Conference, ASME, 1996.

Andresen P. L. "*Effects of Flow Rate on SCC Growth Rate Behavior in BWR Water*", in Proceedings of Eighth International Symposium on Environmental Degradation in Nuclear Power Systems–Water Reactors, Amelia Island, Eds. A. McIlree, S. Bruemmer, American Nuclear Society, pp. 603-614, August 10-14, 1997.

Andresen P. L., "*Stress Corrosion Cracking Testing and Quality Considerations*" in Proceedings of Ninth International Symposium on Environmental Degradation in Nuclear Power Systems – Water Reactors, Eds. S. Bruemmer, F.P.Ford. Published by The Metallurgical Society. ISBN 0-87339-475-5, pp. 411-421, Newport Beach August 1-5, 1999.

Andresen P. L, Gott K. and Nelson J. L., "*Stress Corrosion Cracking of Sensitized Stainless Steel- a Five Lab Round Robin*", in Proceedings of Ninth International Symposium on Environmental Degradation in Nuclear Power Systems – Water Reactors, EdsS. Bruemmer, F.P.Ford. Published by The Metallurgical Society. ISBN 0-87339-475-5, pp. 423-433, Newport Beach August 1-5, 1999a.

Andresen P. L., Ford. F. P., Angeliu T. M. Solomon H. D. and Cowan R. L., "*Prediction of Environmentally- Assisted Cracking and its Relevance to Life Management in BWRs*", in Proceedings of Ninth International Symposium on Environmental Degradation in Nuclear Power Systems – Water Reactors, EdsS. Bruemmer, F.P.Ford. Published by The Metallurgical Society. ISBN 0-87339-475-5, pp. 423-433, Newport Beach August 1-5, 1999b.

Andresen P. L. and Morra M. M., "*SCC of stainless steels and Ni alloys in high temperature water*", Proceedings of NACE Corrosion 2001, TS-E Symposium, Paper #01228, 2001.

Andresen P. L., "*Similarity of Cold Work and Radiation Hardening in Enhancing Yield Strength and SCC Growth of Stainless Steel in Hot Water*", Corrosion/02, Paper 02509, NACE, 2002.

Andresen P. L., Emigh P. E. and Young L. M., "*Mechanistic and Kinetic Role of Yield Strength / Cold Work / Martensite, H_2, Temperature, and Composition on SCC of Stainless Steels*", "Proc. 10th Anniversary INSS Symp. on SCC in Nuclear Power Systems, Osaka, Japan, May 2002.

Andresen P. L., Diaz T. P. and Hettiarachchi S., "*Effect on Stress Corrosion Cracking of Electrocatalysis and Its Distribution Within Cracks*", Proceedings of Eleventh International Conference on Environmental Degradation in Nuclear Power Systems–Water Reactors, Skamania Lodge, Eds. G. Was, L. Nelson, American Nuclear Society, August 5-9, 2003.

Andresen P. L and Morra M. M "*Effects of Positive and Negative dK/da on SCC Growth Rates*", Proc. 12th Int. Symp. on Environmental Degradation of Materials in Nuclear Power Systems – Water Reactors", TMS, Snowbird, pp.167-184, August 2005a.

Andresen P.L.,and Morra M.M. "*Effects of Si on SCC of Irradiated and Unirradiated Stainless Steels and Nickel Alloys*" in Proc. 12th Int. Symp. on Environmental Degradation of Materials in Nuclear Power Systems – Water Reactors", TMS, Snowbird, pp. 87-108, August 2005b.

Andresen P. L. and Morra M. M., "*Effect of Rising and Falling K Profiles on SCC Growth Rates in High Temperature Water*", Journal of Pressure Vessel Technology, Volume 129, Issue 3, pp. 488-506, August 2007a.

Andresen P. L. and Morra M.M., "*Emerging Issues in Environmental Cracking in Hot Water*", in Proceedings of 13th International Conference on Environmental Degradation of Materials in Nuclear Power Systems, Whistler, British Columbia, August 19-23, Sponsored by Canadian Nuclear Society, 2007b.

Andresen P. L. and Morra M. M., "*IGSCC of non-sensitized stainless steels in high temperature water*", Proceedings of 2007 BARC Jubilee Anniversary Conference,. To be published in Journal of Nuclear Materials, 2007c.